Journal of Glaciology (2018), **64**(244) 208–226 doi: 10.1017/jog.2018.8

Controls on rapid supraglacial lake drainage in West Greenland: an Exploratory Data Analysis approach

ANDREW G. WILLIAMSON, IAN C. WILLIS, NEIL S. ARNOLD, ALISON F. BANWELL

Scott Polar Research Institute, University of Cambridge, Cambridge, UK
Correspondence: A.G. Williamson <agw41@cam.ac.uk>

ABSTRACT. The controls on rapid surface lake drainage on the Greenland ice sheet (GrIS) remain uncertain, making it challenging to incorporate lake drainage into models of GrIS hydrology, and so to determine the ice-dynamic impact of meltwater reaching the ice-sheet bed. Here, we first use a lake area and volume tracking algorithm to identify rapidly draining lakes within West Greenland during summer 2014. Second, we derive hydrological, morphological, glaciological and surface-mass-balance data for various factors that may influence rapid lake drainage. Third, these factors are used within Exploratory Data Analysis to examine existing hypotheses for rapid lake drainage. This involves testing for statistical differences between the rapidly and non-rapidly draining lake types, as well as examining associations between lake size and the potential controlling factors. This study shows that the two lake types are statistically indistinguishable for almost all factors investigated, except lake area. Thus, we are unable to recommend an empirically supported, deterministic alternative to the fracture area threshold parameter for modelling rapid lake drainage within existing surface-hydrology models of the GrIS. However, if improved remotely sensed datasets (e.g. ice-velocity maps, climate model outputs) were included in future research, it may be possible to detect the causes of rapid drainage.

KEYWORDS: Arctic glaciology, melt - surface, remote sensing, snow/ice surface processes

1. INTRODUCTION AND AIMS

Many supraglacial lakes (hereafter 'lakes') that form annually within the ablation zone of the Greenland ice sheet (GrIS) drain in the mid- to late season, while others simply freeze in the autumn (Selmes and others, 2013; Tedesco and others, 2013; Miles and others, 2017). Draining lakes can be classified as either 'rapidly' or 'slowly' draining (Chu, 2014; Nienow and others, 2017). Rapid events occur in situ over hours to several days by a hydraulically-driven fracture mechanism ('hydrofracture') (e.g. Das and others, 2008; Doyle and others, 2013; Tedesco and others, 2013; Stevens and others, 2015), with ~10% of lakes thought to drain in this way across the whole GrIS (Selmes and others, 2011, 2013). Slow events occur over days to weeks when a lake overflows and incises a surface outlet stream (Hoffman and others, 2011; Tedesco and others, 2013). Although the two processes are distinct, they can influence each other if, for example, a stream from a slowly draining lake is tapped by a moulin, directing surface water to the ice-sheet bed, and causing uplift or basal sliding that may then induce hydrofracture and rapid drainage nearby (Tedesco and others, 2013; Stevens and others, 2015).

All lakes affect the GrIS's mass balance because they have a lower albedo than the surrounding bare ice, enhancing surface ablation (Lüthje and others, 2006; Tedesco and Steiner, 2011; Tedesco and others, 2012). However, draining lakes, and particularly those draining rapidly, are of additional interest because they affect ice velocities via the delivery of large meltwater volumes to the ice-sheet bed (e.g. Zwally and others, 2002; van de Wal and others, 2008; Schoof, 2010; Colgan and others, 2011a; Cowton and others, 2013; Fitzpatrick and others, 2013; Bougamont and others, 2014 Dow and others, 2014). These meltwater pulses can overwhelm the capacity of the subglacial drainage system, lower subglacial effective pressure, enhance basal sliding and increase surface ice velocity by >200% of background winter levels over short (hourly–daily) timescales (Shepherd and others, 2009; Schoof, 2010; Hoffman and others, 2011; Bartholomew and others, 2011a,b, 2012; Banwell and others, 2013; Tedesco and others, 2013; Andrews and others, 2014; Bougamont and others, 2014; Kulessa and others, 2017). Hydrofracture events also open up moulins that can consequently transport surface meltwater to the bed, potentially promoting sliding over longer (weekly–seasonal) timescales (Zwally and others, 2002; Joughin and others, 2008, 2013; Bartholomew and others, 2010; Colgan and others, 2011b; Palmer and others, 2011; Banwell and others, 2013, 2016; Cowton and others, 2013; Sole and others, 2013; Tedstone and others, 2014; Koziol and others, 2017). This moulin opening is particularly important because cold-based ice at central depths of the GrIS acts as a thermal barrier to water penetration, likely meaning that water can reach the ice bed only through such fractures (Irvine-Fynn and others, 2011; Lüthi and others, 2015; Greenwood and others, 2016; Poinar and others, 2017).

There is debate, however, over the significance of such drainage-driven speed-up over longer (seasonal–decadal) timescales, since the subsequent evolution of subglacial conduits to hydraulically efficient conditions may increase subglacial effective pressures sufficiently to reduce ice velocities, thus offsetting the impact of the earlier speed-ups (Palmer and others, 2011; Sundal and others, 2011; Bartholomew and others, 2011a; Banwell and others, 2013, 2016; Chandler and others, 2013; Andrews and others, 2014; Mayaud and others, 2014; Tedstone and others, 2014, 2015). Finally, rapid lake drainage can affect ice dynamics through the input of relatively warm surface

https://doi.org/10.1017/jog.2018.8 Published online by Cambridge University Press

water to the colder ice beneath, promoting faster ice flow due to the strong dependency of ice-deformation rates on ice temperature (Phillips and others, 2010, 2013), although the significance of this process is debated (Poinar and others, 2017).

To date, most of the above phenomena have been studied for ice-marginal regions of the GrIS, typically below ~1600 m ice-surface elevation. However, recent research has started to examine whether similar processes might extend to the interior regions of the GrIS in the future as surface melt rates increase and lakes form at higher elevations (Liang and others, 2012; Howat and others, 2013; Doyle and others, 2014; Fitzpatrick and others, 2014; Leeson and others, 2015; Poinar and others, 2015; Gledhill and Williamson, 2018). Whether or not there is an altitudinal limit to rapid lake drainage, due to the thicker ice and limited crevassing that may impede hydrofracture, is currently unknown (Poinar and others, 2015). If hydrofracture can occur at these elevations, it seems probable that rapid lake drainage and the subsequent input of meltwater via moulins will cause sustained ice speed-ups over seasonal to annual timescales. This would be likely due to enhanced ice deformation via ice-sheet warming (Phillips and others, 2010, 2013), and enhanced basal sliding due to the thick ice (promoting high creep-closure rates) and low ice-surface slopes (producing low subglacial hydraulic-potential gradients) restricting the evolution of subglacial drainage from distributed to channelised (Meierbachtol and others, 2013; Dow and others, 2014; Doyle and others, 2014; Poinar and others, 2015).

It is essential, therefore, to understand the present distribution of rapid lake-drainage events and the factors that may control the hydrofracture process across the GrIS. If this were better understood, the location, timing and magnitude of rapid lake-drainage events could be incorporated with an improved physical basis into coupled hydrology-ice flow models of the GrIS, which could then be used to predict future ice-sheet dynamics with greater certainty. So far, research into rapid lake drainage has involved fieldwork (Das and others, 2008; Doyle and others, 2013; Tedesco and others, 2013; Stevens and others, 2015), numerical modelling (Banwell and others, 2012, 2013, 2016; Clason and others, 2012, 2015; Arnold and others, 2014; Koziol and others, 2017) or satellite remote sensing (Box and Ski, 2007; Sundal and others, 2009; Selmes and others, 2011, 2013; Liang and others, 2012; Johansson and others, 2013; Morriss and others, 2013; Fitzpatrick and others, 2014; Everett and others, 2016; Chen and others, 2017; Cooley and Christoffersen, 2017; Miles and others, 2017; Williamson and others, 2017).

Collectively, this research has produced a consensus on the general controls on rapid lake drainage for different regions of the GrIS: rapid drainage typically occurs at progressively higher elevations over the melt season, with the usually smaller ice-marginal lakes draining before the larger ones further inland. Currently, several factors thought to control hydrofracture are used to explain rapid lake drainage since it is generally acknowledged that for a fracture to propagate from the ice-sheet surface to the bed, it must remain water-filled for its entire depth (Alley and others, 2005; van der Veen, 2007; Tsai and Rice, 2010). This suggests that a critical water-volume threshold may be needed to initiate rapid lake drainage, with the value of this threshold necessarily being higher for thicker ice. Modelling studies therefore link water volume and local ice thickness to calculate 'fracture area' thresholds for rapid lake drainage, where rapid drainage is triggered once a lake's water volume exceeds the local ice thickness multiplied by a prescribed map-plane fracture area (Clason and others, 2012, 2015; Banwell and others, 2013, 2016; Arnold and others, 2014; Koziol and others, 2017). The underlying physical basis to the fracture area threshold is that the quantity of surface meltwater controls a fracture's filling and expansion, as well as ensuring that it remains open by offsetting refreezing (van der Veen, 2007; Krawczynski and others, 2009). However, these models typically display an equally high performance for a variety of water-volume thresholds (Table 1). It is possible, therefore, that water volume may be important in controlling hydrofracture but only if one or more additional controls work alongside it. For example, field data from Stevens and others (2015) suggest that a local stress perturbation (caused by the delivery of meltwater to the ice-sheet bed via a nearby moulin) is required to initiate hydrofracture, with a certain lake area or volume being only a prerequisite for, rather than the driver of, drainage. However, this study was limited to a single lake (meaning it is unclear whether similar processes operate elsewhere) and it did not examine the potential influence of other controls apart from this, such as those we identify later (Table 2). Moreover, theoretical, field-based, remote sensing and modelling studies have shown that rapidly draining lakes, as well as containing a wide variety of water volumes prior to drainage, have seemingly no common characteristics among the factors that might be influential in causing rapid drainage (Table 1).

Taken together, existing work shows no agreement on the precise hydrological or glaciological controls on rapid lake drainage (notably the required lake area, volume or depth, or the ice-stress regime), with the possibility that the controls vary between lakes and between or within different sectors of the GrIS (for example, between land- and marine-terminating outlets, or interior and ice-marginal regions). There is a need, therefore, to investigate whether the observations from individual lakes apply more widely, whether additional controls are important in driving lake drainage, and whether the controls are spatiotemporally uniform or variable between sectors of the GrIS and times of the year. Towards this end, Selmes (unpublished 2011 Swansea University Ph.D. thesis) examined how ice-sheet thickness, ice-surface slope and ice-surface velocity may influence rapid lake drainage identified from MODIS imagery over the entire GrIS in 2005–09, but found statistically insignificant relationships for all the controls investigated. The study may have been compromised, however, because: (i) the data were of coarse (~5 km) resolution; (ii) the study was over the entire GrIS rather than for specific regions, making patterns difficult to recognise; (iii) the statistical relationships were computed with respect only to lake areas and not lake volumes, and; (iv) the analysis was restricted to linear correlation.

To address the limited previous work, our objective here is to examine the hydrological and glaciological controls on rapid lake drainage suggested by previous research, as well as to examine a variety of other factors that may also control the location, timing and magnitude of rapid lake drainage. This objective is addressed using rigorous, regional-scale statistical Exploratory Data Analysis (EDA), which is an approach to explore existing hypotheses, to

https://doi.org/10.1017/jog.2018.8 Published online by Cambridge University Press

Table 1. Hydrological, glaciological and other notable characteristics of rapidly draining lakes on the GrIS identified in previous studies

Study	Study type	Lake area	Lake volume	Lake depth	Ice thickness	Ice-stress regime	Other drainage controls
		km^2	$10^6\ m^3$	m	km		
Alley and others (2005)	Theoretical	–	–	–	–	High horizontal tension required	Crack must be connected to water body to offset water refreezing
van der Veen (2007)	Theoretical	–	–	–	–	Tension assumed*	Crack propagation speed strongly controlled by meltwater inflow rate
Krawczynski and others (2009)	Theoretical	0.0491	0.098†	2.0–5.0	1.0	No longitudinal stress	–
Boon and Sharp (2003)‡	Theoretical	–	–	7.0	0.15	–	–
Das and others (2008)	Field	5.6	40.4	–	–	–	–
Doyle and others (2013)	Field	4.5	7.4			Compressive lake basin	–
Tedesco and others (2013)	Field	–	1.6	5.0	–	–	–
Stevens and others (2015)	Field	–	7.0§		–	Extension observed	–
Box and Ski (2007)||	Remote sensing	1.4	4.1¶	6.1	–	–	–
Fitzpatrick and others (2014)	Remote sensing	–	–	–	–	–	Nearby rapid lake drainage can incite other rapid drainage events
Miles and others (2017)	Remote sensing	0.0495**	–	–	–	–	–
Williamson and others (2017)	Remote sensing	–	0.3††	–	1.0	–	–
Banwell and others (2013)	Modelling	–	1.0‡‡,††	–	1.0	–	–
Arnold and others (2014)	Modelling	–	4.0–7.5§§,††	–	1.0	–	–
Clason and others (2015)	Modelling	–	–	–	–	Tensile stress ignored	–
Koziol and others (2017)	Modelling	–	2.0–6.0||||,††	–	1.0	–	–

* Theoretical work was insensitive to assumed tension value.
† Calculated by multiplying the study's lower lake-water-depth bound (2 m) by the lower lake-area bound (a 0.25 km-diameter lake approximated as a perfect circle).
‡ Study on John Evans glacier, Ellesmere Island, Canada, rather than the GrIS, but also for cold-based ice (at ~ −10 °C).
§ Study assumes value based on summer 2011 measurements.
|| Study identifies only 'outburst' events, but does not determine the mechanism of 'outburst' (either lake overtopping or hydrofracture).
¶ Smallest value listed in the study, which only presented the 50 largest events.
** Lower bound, limited to the smallest lake size (55 × 30 m pixels = 0.0495 km^2) tracked in the study.
†† Value calculated by multiplying the study's fracture area threshold by an ice thickness of 1 km.
‡‡ Value producing best match between modelled and observed proglacial discharge.
§§ Value producing best match between modelled and satellite-observed (Landsat 7 ETM+) volumes, but volumes were likely overestimated (Pope and others, 2016).
|||| Model sensitivity tested within this range to show how lakes were partitioned into different drainage types based on adjusting this value.

Table 2. Potential controlling factors on hydrofracture investigated in this study. Hydrological and morphological data are at the individual lake scale (i.e. kilometres to several kilometres), glaciological data are at the scale of the ice underlying or adjacent to lakes (i.e. kilometres to tens of kilometres), while surface-mass-balance (SMB) data cover synoptic-scale meteorological processes that typically operate across the entire regions (i.e. tens of kilometres)

Data category	Potential controlling factor	Dimensions	Data source or method	Notes
Hydrological	Lake area	km^2	Williamson and others (2017)	RMSE: 0.323 km^2
Hydrological	Lake volume	m^3	Williamson and others (2017)	RMSE: 5.9×10^7 m^3
Hydrological	Mean lake water depth	m	Williamson and others (2017)	RMSE: 0.29 m
Hydrological	Maximum lake water depth	m	Williamson and others (2017)	RMSE: 0.29 m
Hydrological	Std dev. of lake water depth (in space)	m	Williamson and others (2017)	
Hydrological	Lake mean filling rate	$m^3\ s^{-1}$	Williamson and others (2017)	Over previous 5 days
Morphological	Lake eccentricity	–	Banwell and others (2014)	
Morphological	Lake orientation	°	Banwell and others (2014)	W.r.t. ice-flow direction*
Glaciological	Ice-surface elevation	m a.s.l.	Howat and others (2014)	At lake's centroid
Glaciological	Ice-bed elevation	m a.s.l.	Morlighem and others (2014)	At lake's centroid
Glaciological	Ice-sheet thickness	m	Ice surface minus bed elevation	At lake's centroid
Glaciological	Ice-surface slope†	°	ArcGIS 'Slope' tool	Across lake basin‡
Glaciological	Background winter ice velocity	$m\ a^{-1}$	Joughin and others (2010, 2016)	Across lake basin
Glaciological	Principal ice-surface strain rate	a^{-1}	Poinar and others (2015)	Across lake basin
Glaciological	von Mises yield criterion	Pa	Clason and others (2015)	Across lake basin
SMB	Melt within catchment§ on day	mm w.e.	Noël and others (2016)	
SMB	Melt within catchment on previous day	mm w.e.	Noël and others (2016)	
SMB	Rain within catchment on day	mm w.e.	Noël and others (2016)	
SMB	Rain within catchment on previous day	mm w.e.	Noël and others (2016)	
SMB	Cumulative melt in catchment	mm w.e.	Noël and others (2016)	
SMB	Cumulative rain in catchment	mm w.e.	Noël and others (2016)	
SMB	Cumulative runoff in catchment	mm w.e.	Noël and others (2016)	Melt plus rain
SMB	Difference between cumulative catchment runoff and lake volume	m^3		Runoff minus volume

* Average ice flow derived from *x* and *y* components of MEaSUREs winter velocity data.
† Derived from ice-surface elevation data, which were first coarsened to 1 km resolution to ensure slopes were derived across rather than within lake basins, then interpolated (using a nearest-neighbour technique) to 250 m resolution for consistency with the other data.
‡ Lake basin is defined as the lake area at the lake's maximum extent (for non-rapidly draining lakes) or on the day prior to hydrofracture (for rapidly draining lakes).
§ Catchment refers to a lake's ice-surface catchment, determined with MATLAB's 'watershed' function (using a default eight-connected neighbourhood).

re-evaluate them with new data and perhaps to propose new hypotheses or to suggest future research directions (Tukey, 1977). The EDA focuses on two locations: the land-terminating Paakitsoq and the marine-terminating Store Glacier regions of West Greenland (Fig. 1), for the 2014 melt season. We conduct this analysis for a large sample of 213 lakes to determine whether the insights gained from previous field studies (e.g. Doyle and others, 2013; Tedesco and others, 2013; Stevens and others, 2015) for individual lakes more widely apply. The EDA aims to:

1. Identify the distribution of rapidly and non-rapidly draining lake types within the two regions, including their areas, volumes and their drainage dates or the dates when they reach their maximum extent.
2. Derive data for a variety of potential controlling factors that may explain the observed distributions of the lake types within the regions.
3. Analyse whether there are statistically significant *differences* between the two lake types in terms of the potential controlling factors.
4. Analyse whether statistically significant *correlations* exist between the potential controlling factors and both lake areas or volumes for the two lake types.

Collectively, the above analysis might indicate links between one or multiple factors and the incidence of hydrofracture on the GrIS.

2. METHODS, DATA AND STUDY SITES

Here, we describe: (i) the methods used to identify rapidly and non-rapidly draining lakes (Section 2.1); (ii) the original datasets used in the EDA, and the derivation of various factors from these data that may control the spatiotemporal patterns of rapid lake drainage, including the justification for including them (Section 2.2); (iii) the statistical techniques for the EDA (Section 2.3); and, (iv) the rationale for choosing the study sites (Section 2.4).

2.1. Identifying rapidly and non-rapidly draining lakes

For the first aim of the study, involving detecting rapid lake-drainage events and thus the distribution of rapidly draining and non-rapidly draining lakes, we used the Fully Automated Supraglacial lake Tracking (FAST) algorithm (Williamson and others, 2017). Images derived from the MODIS MOD09 surface-reflectance product from 1 May to 30 September 2014 were chosen, totalling 153 images. Bands 1 (red; 0.620–0.670 μm) and 6 (1.628–1.652 μm) were required; band-1 data are distributed at native ~250 m resolution, while band-6 data have ~500 m resolution. We chose MODIS imagery to exploit the daily temporal resolution of the record, crucial for identifying rapid lake drainage since hydrofracture occurs in hours to days, although we recognised there was a trade-off with MODIS's lower spatial resolution (Leeson and others, 2013; Miles and others, 2017; Williamson and others, 2017).

https://doi.org/10.1017/jog.2018.8 Published online by Cambridge University Press

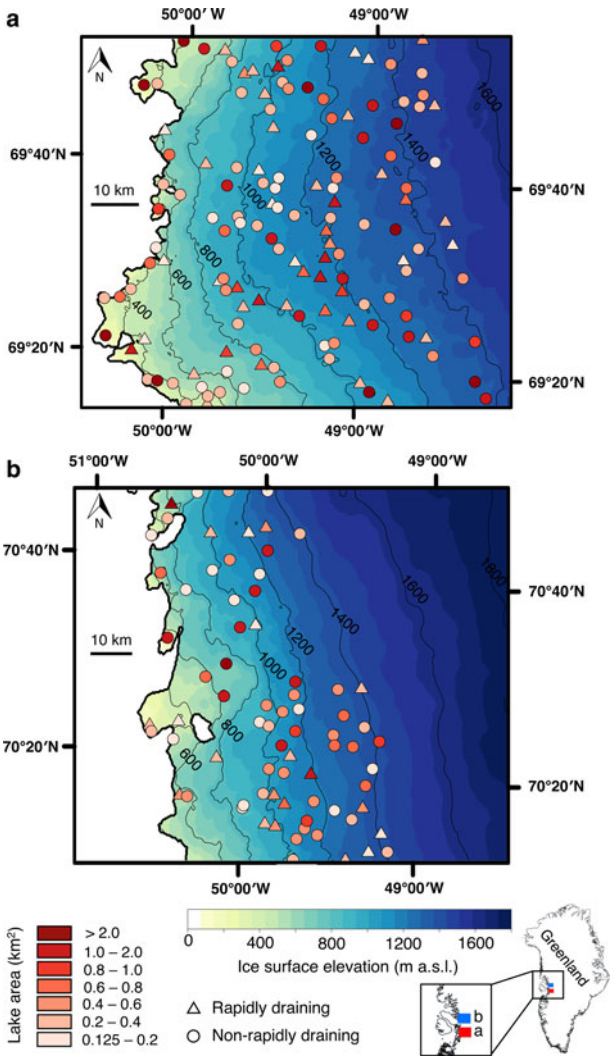

Fig. 1. The (a) Paakitsoq and (b) Store Glacier regions of West Greenland (inset). Note the difference in horizontal scale between the two panels. Polygons indicate whether lakes observed in 2014 MODIS imagery drain rapidly (triangles; ⩽4 days) or not (circles; >4 days), colour-coded according to area immediately prior to drainage for rapidly draining lakes and area when reaching their maximum seasonal extents for non-rapidly draining lakes (see Section 3.1). The GrIS margin (thick black line) and ice-surface elevation contours (thin black lines) from Howat and others (2014) are shown.

Williamson and others (2017) provide full details of the FAST algorithm, but, briefly, it incorporates the following steps:

1. MODIS images are pre-processed using the MODIS Reprojection Tool Swath (version 2.2), including reprojection to the Polar Stereographic grid (EPSG: 3413) using bilinear interpolation, and sharpening of band-6 data from 500 m resolution to match band 1's 250 m resolution.
2. MODIS tiles are cropped automatically to the study regions using a georeferenced mask, ice-marginal areas are removed using the Greenland Ice Mapping Project ice-sheet mask (Howat and others, 2014), and clouds and cloud shadows are filtered when band-6 values exceed 0.15.
3. Lake areas are derived for each image using dynamic thresholding of the red band. This approach identifies a water-covered pixel when the reflectance of the central pixel in a 25 × 25-pixel moving window is below 0.640 of the mean red-band reflectance within the whole window. MODIS lake areas derived by this method have a RMSE of 0.323 km^2 (~5 MODIS pixels) when compared with lake areas delineated from a supervised classification of higher-resolution Landsat 8 Operational Land Imager (OLI) imagery (Williamson and others, 2017; their fig. 6).
4. Lake depths and volumes are calculated within the boundaries of each lake on each image with Sneed and Hamilton's (2007) physically-based method applied to the red band, using the parameters and methods outlined in Williamson and others (2017). The RMSEs for MODIS lake depths and volumes are, respectively, 1.27 m and 5.9×10^7 m^3 when compared with values derived from applying the same method to Landsat 8 imagery (Williamson and others, 2017; their fig. 10).
5. The binary masks depicting lake areas for each image are superimposed to create a mask showing the maximum summer extent of all lakes. Within this mask, changes to individual lake areas and volumes across each consecutive image pair are then tracked, with cloud-obscured lakes marked as no-data values. To reduce the error associated with misclassifying a single pixel as water, lakes that do not grow to at least two MODIS pixels (i.e. 0.125 km^2) at least once in the season are excluded.
6. Rapid lake-drainage events are identified when a lake loses ⩾80% of its maximum seasonal volume over ⩽4 days. While hydrofracture typically occurs in ⩽2 days (e.g. Das and others, 2008; Doyle and others, 2013; Tedesco and others, 2013), the threshold is relaxed to compensate for missing data within the satellite record due to false negatives and cloud cover. This threshold is more stringent than that used for remotely identifying rapid lake drainage by Morriss and others (2013; 6 days) and identical to that assumed by Fitzpatrick and others (2014; 4 days). Following Liang and others (2012), rapid lake-drainage events are deemed false positive if the basin refills within 7 days of an event termination. The dates of drainage initiation, together with the lake water volumes immediately prior to drainage, are derived for all of the rapid events.

Two lake types were recognised by the procedure outlined above: lakes that drained rapidly at least once in the season, and non-rapidly draining lakes, which included lakes that: (i) drained slowly (losing ⩽80% of their maximum seasonal water volume over ⩽4 days or losing any water volume over ⩾4 days); (ii) did not drain but simply froze towards the end of the melt season, and; (iii) were falsely classified as non-rapidly draining by the FAST algorithm due to cloud cover or false negatives within the MODIS record. Since Williamson and others (2017) extensively tested the outputs from the FAST algorithm against Landsat 8 OLI imagery (regarded as ground-truth data) for 2014 in the study regions, we are confident in the data used here, including in the correct identification of rapid lake drainage.

2.2. Deriving potential controlling factors on rapid lake drainage

For the second aim of the research, we acquired other datasets to calculate 21 additional factors that may potentially

https://doi.org/10.1017/jog.2018.8 Published online by Cambridge University Press

control rapid lake drainage besides just their areas and volumes (Table 2). The 23 factors were separated into four categories: (i) hydrological, (ii) morphological, (iii) glaciological, and (iv) SMB. Time-dependent factors were derived for the day of hydrofracture initiation for the rapidly draining lakes and for the day when the lake reached its maximum seasonal extent for the non-rapidly draining lakes. The motivations for exploring these factors, along with the methods for their derivation, are outlined in the following sections.

2.2.1. Hydrological factors

Six hydrological factors (Table 2) were derived with the FAST algorithm (Section 2.1). The rationale for including them is that previous research has suggested a possible link between rapid lake drainage and the lake's area, volume, depth, or some combination thereof. The std dev. of lake water depth (in space) was included to investigate whether lakes with a more uniform depth were more likely to fracture and drain rapidly than those containing more variable depths (such as having a few locations with very deep water). The lake's mean filling rate was included due to the potential link between the rate of increase in the hydrostatic pressure head and the timing and/or occurrence of hydrofracture (e.g. van der Veen, 2007). For example, Tedesco and others (2013) showed that a lake drained rapidly following an increased filling rate due to an overflowing upstream lake, although it is plausible that the lake's drainage simply resulted from the increased water volume within it.

2.2.2. Morphological factors

Two morphological factors, lake eccentricity and orientation (Table 2), were derived using MATLAB's 'regionprops' function, which involved best-fitting an ellipse to the lake outline, as described in Banwell and others (2014; their fig. 1). The eccentricity is a ratio that describes how closely a lake resembles a circle, and the orientation is the angle of the lake's long axis relative to the orientation of the average ice flow (ascertained with the ice-velocity dataset described in Section 2.2.3). These morphological properties were investigated since different patterns of normal stress at the lake bottom (induced by the water) with respect to the surface horizontal stress field of the ice (induced by ice flow) might make it more or less likely for hydrofracture to be initiated.

2.2.3. Glaciological factors

Seven glaciological factors (Table 2) were included to investigate how the properties of the ice, including the horizontal velocity field around a lake (used to calculate the local stress and strain rates), and the local ice-sheet topography, might influence lake-drainage potential. Since high temporal resolution velocity data were unavailable for summer 2014, we used the background (long-term, steady state) winter ice-velocity data from the MEaSUREs multi-year mosaic (Joughin and others, 2010, 2016) to calculate the principal ice-surface strain rate ($\dot{\varepsilon}$) and the von Mises yield criterion (σ_V); for details of the calculations, see the supplementary information. Positive $\dot{\varepsilon}$ values indicate areas of extension, while negative ones indicate compression; higher σ_V values indicate areas undergoing the most tension or where two surface parallel principal stresses are both compressive (Vaughan, 1993; Clason and others, 2015).

2.2.4. SMB factors

To investigate the relation of rapid lake drainage to SMB processes, we used downscaled daily 1 km resolution RACMO2.3 data for the GrIS (Noël and others, 2016) from summer 2014 to derive eight potential SMB controlling factors (Table 2). These data were used to explore whether the quantity of melt and precipitation within a lake's ice-surface catchment influence rapid drainage. This may be important because, for example, Stevens and others (2015) provide evidence that water input through crevasses to the ice-sheet bed at a location proximal to a rapidly draining lake's site is an important precursor to drainage. We assembled melt, rain and runoff data for lake catchments on the day of drainage for rapidly draining lakes and on the day of the lake's maximum extent for non-rapidly draining lakes. We also assembled these data for the day previously, as well as the cumulative seasonal totals up to that point. Finally, we calculated the difference between a lake's volume at its maximum extent (for non-rapidly draining lakes) or on the day prior to its drainage (for rapidly draining lakes) and the cumulative total runoff (i.e. melt plus rain) within the ice-surface catchment up to those dates. The rationale here was that a big discrepancy between these two volumes would imply that large amounts of water might have previously entered the GrIS via crevasses or pre-existing moulins near to the lake, which could have reached the ice-sheet bed, initiating basal uplift or sliding, and thereby increasing the propensity for hydrofracture (e.g. Stevens and others, 2015).

2.3. EDA techniques

For the third and fourth aims of the research, we used the EDA branch of statistical analysis (Tukey, 1977) to explore the existing hypotheses of rapid lake drainage, to re-evaluate them in the context of the new dataset, and perhaps to suggest new ones that better explain the observations (Tukey, 1977). EDA contrasts with confirmatory analysis, which involves testing only specific hypotheses, and deterministic analysis, which involves formulating statistical models. EDA is thus an important analytical step to help determine whether statistical models might be devised from the data, which, in this context, could assist in the formulation of better physically-based models for rapid lake drainage on the GrIS. Here, we used EDA to test for differences (Section 2.3.1) and associations (Section 2.3.2) in the data.

2.3.1. Statistical tests for difference

For the third aim of the study, our analysis involved testing for statistically significant differences between the rapidly draining and non-rapidly draining lake types to determine if the lakes were drawn from the same population. This was partly used to examine whether the potential controls on hydrofracture were able to account for the observed regional distributions of the two lake types. First, we conducted a univariate parametric analysis: this involved a series of unpaired Student's two-sample *t*-tests for each of the potential controlling factors for the two data samples (i.e. rapidly draining and non-rapidly draining lakes), with significance tested at the 95% confidence interval (probability indicator = <0.05) because many data points (213) were involved. None of the data were normally distributed (verified using the Kolmogorov–Smirnov test with 95% confidence) but since the sample size was high (>50) for both the rapidly draining

https://doi.org/10.1017/jog.2018.8 Published online by Cambridge University Press

and non-rapidly draining lake samples, the Student's two-sample *t*-test could be used.

Second, we conducted multivariate principal component analysis (PCA). PCA was used to determine whether the rapidly draining and non-rapidly draining lake types could be distinguished based on a combination of the potential controlling factors (Table 2). PCA removes collinearity between variables in a dataset, collapsing the data into a set of components that show the maximum amount of variance within the data (Jolliffe, 2002), a technique used previously in glaciology, for example, to pre-process different spectral bands of satellite imagery prior to glacier-surface classification (Pope and Rees, 2014a,b) or to map ice flow (Fahnestock and others, 2016). We examined the first three principal components (PCs), with each subsequent PC accounting for progressively decreasing data variance, and positioned orthogonal to the previous PC (Ringnér, 2008). Since the potential controlling variables were measured at different scales and had different dimensions, the data were first normalised and rendered dimensionless using the inverse variable variances as weights. PCA involved two stages: first, it was undertaken separately for each category of factor from Table 2 (i.e. hydrological, morphological, glaciological and SMB) and, second, it was conducted for all the potential controlling factors listed in Table 2 together. During the first step, the morphological factors were grouped with the hydrological factors because there were only two morphological variables and, if they had not been included within another category, they could not have been incorporated into the PCA; furthermore, it was most obvious to group these two categories of controlling factor together since they both represent data collected at the local lake scale. For each stage of analysis, once the individual PCs were identified, the scores for the first three PCs for each lake were determined and projected in the new coordinate space; if the two lake types were statistically different based on the groups of controlling factors, they would be expected to visibly cluster within specific areas of the PCA plots. Finally, for each stage of PCA, this clustering was also assessed quantitatively for the rapidly draining and non-rapidly draining lakes by testing for statistical differences between the first three PCs using unpaired two-sample Student's *t*-tests (verified at the 95% confidence interval).

2.3.2. *Statistical tests for association*

The next part of the EDA, and the fourth element of the study, comprised formulating bivariate linear correlation relationships to determine whether there were statistically significant associations between the lake areas or volumes of rapidly and non-rapidly draining lakes and the other factors, and how these associations differed between the lake types. The objectives here included determining whether a critical lake area or volume was needed for hydrofracture that scaled with any of the other potential controlling factors, and therefore also identifying any linear regression relationships between the various controlling factors, for example to see if greater lake volumes need to be reached for thicker ice or for more compressive ice flow. In addition, we aimed to examine whether different associations existed for the two lake types to help explain any differences in their phenomenological behaviour. Since the data were not normally distributed, the relationships were assessed using the Spearman's rank correlation coefficient (ρ), with statistical significance checked with 95% confidence.

2.4. Study sites

The analysis was conducted for two sites in West Greenland (Fig. 1): (a) the Paakitsoq land-terminating region north of Jakobshavn Isbræ, and (b) the region surrounding Store Glacier, a large, fast-flowing marine outlet glacier. We identified 213 lakes $\geqslant$0.125 km^2 across these two regions in 2014, representing just under 20% of the 1126 lakes mapped with MODIS across the whole of south-west Greenland in 2005–09 (Selmes and others, 2011). This gave us confidence that our sample represented the wider population of lakes. Both regions were similarly sized, extending ~70 km latitudinally, and ~80 km inland, to ensure that the highest-elevation lakes were included in the record. We used data from 2014 as it was a climatically 'normal' year (van den Broeke and others, 2016) without extreme weather that could have affected the applicability of our findings to other times.

3. RESULTS

3.1. Distribution of rapidly draining and non-rapidly draining lakes

The first aim of the study was to identify the distribution of rapidly and non-rapidly draining lakes within the two regions, including their areas, volumes and their drainage dates or the dates when they reach their maximum extent. These results are shown in Figures 1–3, respectively. Within Paakitsoq, we identified 48 rapidly draining and 90 non-rapidly draining lakes, and at Store Glacier, we identified 21 rapidly draining and 54 non-rapidly draining lakes. There was no obvious variation in lake area or volume by elevation band. However, non-rapidly draining lakes seem to have, on average, larger areas than rapidly draining lakes (Fig. 1), even though the volumes appear more similar (Fig. 2); these patterns are verified statistically later (Section 3.2). Figure 3 shows, as in previous studies (e.g. Fitzpatrick and others, 2014; Miles and others, 2017), an up-glacier progression of rapid lake drainage over the season within both study regions although there are exceptions, with some lower-elevation lakes draining uncharacteristically late in the season.

The data from both regions were grouped to form a single large sample of 69 rapidly draining lakes and 144 non-rapidly draining lakes, in order to represent a sample of the entire population of lakes in West Greenland (Selmes and others, 2011). Tables 3 and 4 show that in the case of both ice-surface-elevation and ice-thickness bands for lakes grouped by area and volume, more lakes drained rapidly at a given elevation or ice thickness simply because the total number of lakes in that band was greater. This demonstrates that there is no bias towards rapid lake drainage occurring at certain ice thicknesses or ice-surface elevations. Furthermore, Tables 3 and 4 suggest that there is no association between ice thickness or ice-surface elevation and the area or volume of lakes for both the rapidly and non-rapidly draining types, which is verified statistically later (Section 3.3).

3.2. Differences in potential controlling factors between rapidly draining and non-rapidly draining lakes

The second aim of the study was to gather data for other potentially controlling factors on hydrofracture (Table 2)

https://doi.org/10.1017/jog.2018.8 Published online by Cambridge University Press

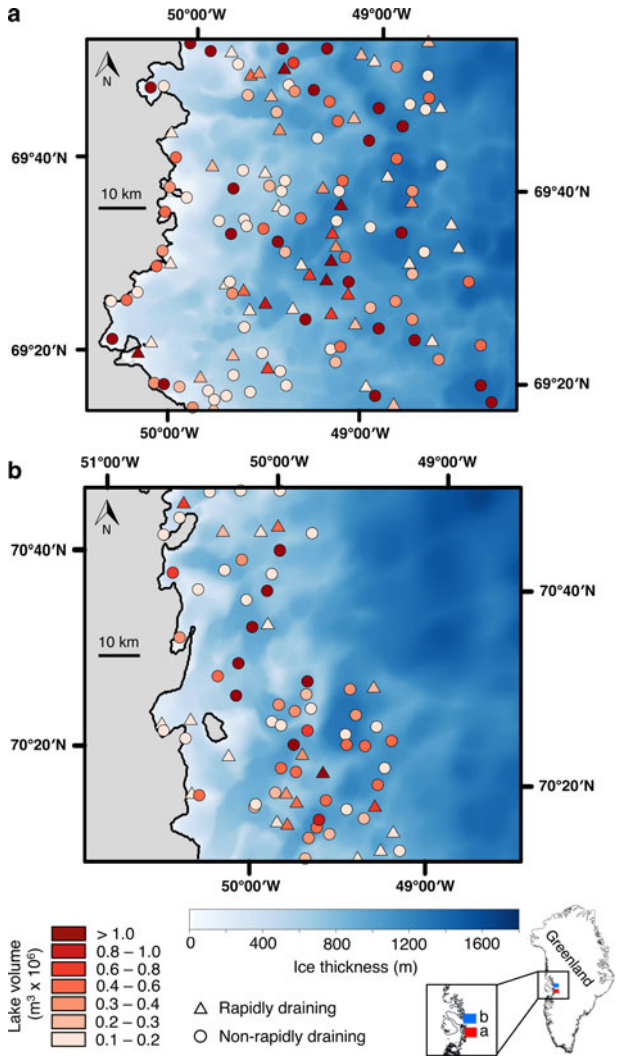

Fig. 2. The locations of rapidly draining (triangles) and non-rapidly draining (circles) lakes within the (a) Paakitsoq and (b) Store Glacier regions of West Greenland (inset) overlying the background ice thickness (m) from Morlighem and others (2014). Colour coding shows lake water volumes immediately prior to drainage for rapidly draining lakes and the water volumes when lakes reached their maximum extent for non-rapidly draining lakes. The thick black lines on both panels delineate the GrIS margin from Howat and others (2014). Note the difference in horizontal scale between the two panels.

and the third aim was to analyse whether these factors could explain the distributions of rapidly draining and non-rapidly draining lakes, and so to examine the differences in the factors between the lake types. First, the two lake types were compared qualitatively using boxplots (Fig. 4) and statistically using unpaired Student's *t*-tests (Table S1). The analysis revealed that the two lake types are indistinguishable for the majority of potential controlling factors. Some factors show a wide spread of values with, in some cases, a high proportion of data falling outside 2.7 σ of the arithmetic mean (for example, lake area, lake volume or the principal strain rate) (Fig. 4), but this pattern is usually observed for both the rapidly draining and non-rapidly draining lake types. For the hydrological factors (Table 2), Figure 4(a) and Table S1 show that the lake types are statistically similar in all cases, except lake area (Fig. 1), where non-rapidly lakes (mean = 0.69 km^2) are statistically larger ($t = -2.261$; $p =$ 0.025) than rapidly draining lakes (mean = 0.47 km^2). For lake volume (Fig. 2), we see a similar pattern, with non-rapidly draining lakes containing higher volumes (mean = 7.4×10^5 m^3) than rapidly draining lakes (mean = 4.1×10^5 m^3), with the difference in lake volume only narrowly missing the 95% interval required for statistical confidence ($p = 0.054$; Table S1). The two lake types are also statistically indistinguishable for the morphological factors (Figs. 4b and 5; Table S1). Among the glaciological factors, including the ice-surface elevation (Fig. 1), the ice-surface slopes (Fig. 5), the ice-bed elevation (Fig. 6), the ice thickness (Fig. 2), the ice-surface principal strain rate (Fig. 7) and the von Mises yield criterion (Fig. 8), the lake types are also indistinguishable (Fig. 4c); Table S1). Thus, there is no evidence for rapidly draining lakes to be located preferentially within thinner or thicker ice (Fig. 2), or within areas undergoing notably high extension or compression (Figs. 7 and 8), with an approximately equal distribution of rapidly draining and non-rapidly draining lakes within these areas. For example, the mean principal strain rate is nearly identical for the two lake types – 0.04 (i.e. slightly compressional) for rapidly-draining lakes and 0.00 for non-rapidly draining lakes (Table S1) – indicating that they are situated within similar strain regimes. Finally, the SMB factors are statistically similar between the two lake types (Figs. 4d and 6; Table S1), with both showing similar patterns of melt, rain, runoff and differences between the cumulative runoff within their catchments and their water volumes.

3.2.1. *Principal component analysis*

Figures S5–S7 show the results of the first step of the PCA, where each category of variable (Table 2) was analysed separately. Figure 9 shows the second step of the PCA, which was performed for all of the variables simultaneously. In every case, the two lake types do not cluster within specific areas of the PCA plots, suggesting that they are not statistically distinguishable. The results of unpaired two-sample Student's *t*-tests for the first three PCs verify the statistically indistinguishable nature of the lake types (Table 5). This shows that the rapidly draining and non-rapidly draining lakes are statistically similar in terms of all of the properties examined; they are thus drawn from the same population.

3.3. Associations between lake area or volume and potential controlling factors

The fourth and final aim of the study was to determine whether there were differences in the associations between lake area or volume and the potential controlling factors for the two lake types, and whether there was a critical threshold for rapid lake drainage that could be linked to one of the other potential controlling factors. Existing modelling studies have only considered this possibility with regard to lake area or volume and the local ice thickness, but found similar model performance for a range of thresholds (Banwell and others, 2013, 2016; Arnold and others, 2014; Koziol and others, 2017). It is plausible, however, that a lake area or volume threshold exists with respect to a factor other than local ice thickness. For example, hydrofracture might occur if a certain lake size is reached *and* a certain strain pattern exists (Fig. 7), with larger (or smaller) sizes required in more compressive (or more tensile) regions. Alternatively, perhaps rapid lake drainage is initiated once

https://doi.org/10.1017/jog.2018.8 Published online by Cambridge University Press

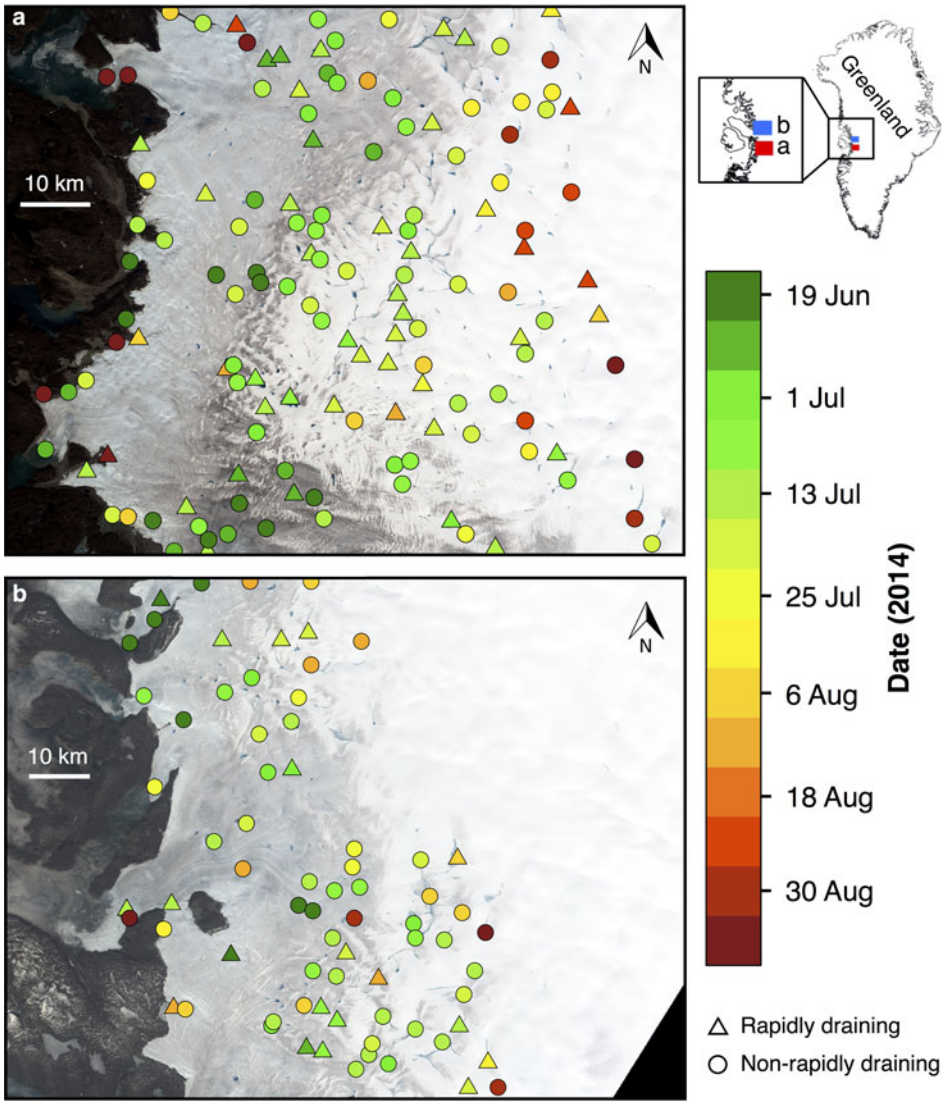

Fig. 3. The dates on which rapidly draining lakes (triangles) drain and the dates on which non-rapidly draining lakes (circles) reach their maximum extents in the (a) Paakitsoq and (b) Store Glacier regions within West Greenland (inset) highlighting the similarity between the two sets of dates. Panels are equivalent to those in Figures 1, 2, 5 and 6. The extreme early and late colour bar values include dates outside of those shown (i.e. from 1 May to 18 June, and from 6 September to 30 September, respectively). Note that most of the lakes shown on the images are included in the analysis, but that some of the smaller lakes are omitted, particularly at Paakitsoq; for further details, see Williamson and others (2017). The backgrounds are true-colour Landsat 8 OLI images from (a) 3 July 2014 (path: 009; row: 011) and (b) 1 July 2014 (path: 011; row: 010). Note the difference in horizontal scale between the two panels.

a certain lake size is attained *and* a particular volume of melt has already been lost from the catchment (Fig. 6), with larger (or smaller) lake sizes required in catchments where less (or more) melt has been lost into the GrIS. Bivariate correlations were examined between both lake areas (Table S3) and lake volumes (Table S4) and the other factors potentially controlling hydrofracture. The results in Tables S3 and S4 show that the majority of the correlations are statistically insignificant, indicating no link between these variables and lake area and volume. However, Table 6 presents results for the correlations that were statistically significant at above the 95% confidence interval. For rapidly draining lakes, the only significant correlation is between lake area and ice-bed elevation, but for the non-rapidly draining lakes there were more numerous significant correlations (Table 6). Tables S3 and S4 also show strong correlations between lake areas or volumes (for both rapidly draining and non-rapidly draining lakes) and the other hydrological factors, notably the maximum, mean and std dev. of lake depth, and the lake filling rate, but these are not included within Table 6 since it seems obvious that these variables should be correlated with lake area or volume.

4. DISCUSSION

Collectively, our results show that rapidly draining and non-rapidly draining lakes for these two regions of the GrIS are largely indistinguishable in terms of the potential hydrofracture controlling factors examined here (Sections 3.1 and 3.2). This suggests that, in statistical terms, the lakes are drawn from the same population. Moreover, when the lakes are categorised according to their mode of drainage, the correlation analysis is unable to explain nearly all of the variability of lake area or volume for the rapidly draining lakes (except when ice-bed elevation was the independent variable), but can explain some of the variability for non-rapidly draining lakes (Section 3.3). Here, we first discuss the likely reasons for the results of the correlation analyses (Section 4.1); second, we examine the results of the

https://doi.org/10.1017/jog.2018.8 Published online by Cambridge University Press

Table 3. Distribution of rapidly draining (RD) and non-rapidly draining (NRD) lakes by ice-surface-elevation and ice-thickness bands, with lakes grouped according to their areas. These data are presented as grouped bar charts in Figures S1 and S2

Ice-surface elevation (m a.s.l.)	Lake area (km^2)														
	0.125–0.2		0.2–0.4		0.4–0.6		0.6–0.8		0.8–1.0		1.0–2.0		>2.0		
	RD	NRD	RD	NRD	RD	NRD	RD	NRD	RD	NRD	RD	NRD	RD	NRD	Total
<400	1	2	4	7	–	–	–	2	–	1	1	1	–	3	22
400–600	2	2	1	4	1	1	–	3	–	–	–	2	1	1	18
600–800	1	3	1	3	–	1	–	1	1	–	–	–	–	1	12
800–1000	2	8	8	11	3	6	–	1	1	1	2	3	–	–	46
1000–1200	3	7	3	7	2	11	4	1	1	2	3	7	–	2	53
1200–1400	5	4	5	6	2	6	1	7	–	2	1	5	–	3	47
>1400	2	1	3	5	1	2	–	–	–	1	–	–	–	–	15
Total	16	27	25	43	9	27	5	15	3	7	7	18	1	10	213
	Lake area (km^2)														
Ice thickness (m)	0.125–0.2		0.2–0.4		0.4–0.6		0.6–0.8		0.8–1.0		1.0–2.0		>2.0		
	RD	NRD	RD	NRD	RD	NRD	RD	NRD	RD	NRD	RD	NRD	RD	NRD	Total
<200	3	3	3	6	1	1	–	2	–	2	1	2	–	2	26
200–400	1	1	4	6	–	–	–	1	–	–	–	–	–	2	15
400–600	1	1	2	2	–	1	–	2	1	–	–	2	1	–	13
600–800	3	11	6	10	4	6	2	1	1	1	1	3	–	1	50
800–1000	4	8	6	8	1	11	1	1	1	1	2	6	–	1	51
1000–1200	2	2	6	7	3	4	2	3	–	4	2	3	–	1	39
>1200	2	1	–	2	–	4	1	4	–	–	1	2	–	3	20
Total	16	27	27	41	9	27	6	14	3	8	7	18	1	10	213

statistical tests for difference for each category of potential controlling factor, with reference to existing hypotheses for rapid lake drainage (Section 4.2), and; finally, we discuss the potential explanations for the negative results of this study and suggest where future research should be directed (Section 4.3).

4.1. Associations between lake area or volume and potential controlling factors

When all of the lakes within both study regions were categorised according to their drainage mode, and then examined using a series of tests for correlation, the results indicate that, for rapidly draining lakes, the lakes normally drain before we observe that any of the controls are influential, whereas some of the controls are influential for the non-rapidly draining lakes. The negative weak correlation (Table 6) for both lake types between ice-bed elevation and lake area suggests that larger lakes tend to form in areas of lower ice-bed elevation, likely because the bed tends to be lower inland where the larger area lakes are present (Figs. 1 and 6). The weak positive correlation (Table 6) between ice thickness and non-rapidly draining lake area and volume can be explained because non-rapidly draining lakes grow bigger inland where the ice is thicker. This observation was also supported by the weak negative correlation (Table 6) between ice-surface slopes and non-rapidly draining lake volume since ice-surface slopes are lower inland (Fig. 5), meaning non-rapidly draining lakes can reach higher volumes here than closer to the coast, where the steeper ice-surface slopes prevent the formation of the largest lakes. These correlation results might also be because lakes tend to form over relatively low areas of bed topography (Lampkin and VanderBerg, 2011; Sergienko, 2013). The lack of similar correlations between rapidly draining lake areas or volumes and the same factors indicates that ice thickness is not important in determining the size of the rapidly draining lakes prior to their drainage, instead suggesting that another factor may drive their rapid drainage. Non-rapidly draining lake volume also decreases as lakes become more eccentric (i.e. less circular and more linear; Fig. 5), and so the lakes will contain lower total water volumes, possibly because the more linear features occur higher on the ice sheet where lakes are bigger (Fig. 1), which could include some areas of slush rather than water contained within lakes. Finally, the correlation analysis shows that the cumulative totals of melt, rain and runoff in non-rapidly draining lake catchments are important in controlling the size of these lakes (Table 6), as we would expect. However, the lack of a similar relationship between these SMB factors and rapidly draining lakes may be because these factors are not important for affecting the size of these lakes.

4.2. Statistically similar rapidly draining and non-rapidly draining lakes

4.2.1. Hydrological factors

Among all factors examined, this category was the only one for which any difference between the two lake types was identified: non-rapidly draining lakes are, on average, more expansive than rapidly draining lakes ($p < 0.05$); with slightly reduced confidence ($p = 0.054$), they also contain larger water volumes. Existing models of the GrIS's hydrology use a critical threshold for lake area or volume, scaled with local ice thickness, to predict hydrofracture (Banwell and

https://doi.org/10.1017/jog.2018.8 Published online by Cambridge University Press

Table 4. Distribution of rapidly draining (RD) and non-rapidly draining (NRD) lakes by ice-surface-elevation and ice-thickness bands, with lakes grouped according to their water volumes. These data are presented as grouped bar charts in Figures S3 and S4

Ice-surface elevation (m a.s.l.)	Lake volume (10^6 m^3)														
	0.1–0.2		0.2–0.3		0.3–0.4		0.4–0.6		0.6–0.8		0.8–1.0		>1.0		
	RD	NRD	RD	NRD	RD	NRD	RD	NRD	RD	NRD	RD	NRD	RD	NRD	Total
<400	3	6	2	–	–	4	–	3	–	–	1	1	1	3	24
400–600	4	4	–	1	–	1	–	3	1	1	–	–	–	3	18
600–800	3	5	2	–	–	–	–	–	1	–	–	–	–	1	12
800–1000	6	15	3	6	2	3	3	1	–	–	1	–	1	5	46
1000–1200	3	9	2	5	3	3	1	8	4	2	–	1	3	9	53
1200–1400	7	9	2	2	2	7	1	7	1	–	–	–	1	8	47
>1400	4	6	–	–	–	–	–	3	–	–	–	–	–	–	13
Total	30	54	11	14	7	18	5	25	7	3	2	2	6	29	213
	Lake volume (10^6 m^3)														
Ice thickness (m)	0.1–0.2		0.2–0.3		0.3–0.4		0.4–0.6		0.6–0.8		0.8–1.0		>1.0		
	RD	NRD	RD	NRD	RD	NRD	RD	NRD	RD	NRD	RD	NRD	RD	NRD	Total
<200	7	5	–	–	–	5	–	4	–	–	–	–	1	3	25
200–400	2	6	3	1	–	–	–	1	–	–	–	–	–	2	15
400–600	2	4	2	–	–	–	–	1	1	1	–	–	–	2	13
600–800	6	18	1	5	3	2	5	2	1	1	–	–	1	5	50
800–1000	6	11	2	5	2	5	–	6	3	1	1	–	1	8	51
1000–1200	5	6	5	3	1	3	–	7	2	–	–	1	2	4	39
>1200	2	4	–	–	1	3	–	4	–	–	–	–	1	5	20
Total	30	54	13	14	7	18	5	25	7	3	1	1	6	29	213

others, 2013, 2016; Arnold and others, 2014; Clason and others, 2015; Koziol and others, 2017). However, our results show that, in many places, non-rapidly draining lakes were able to expand without causing hydrofracture to a size that was larger than that which caused hydrofracture elsewhere. Thus, while these current models assume a certain lake area or volume triggers hydrofracture, which could indicate that rapidly draining lakes would be larger than non-rapidly draining lakes, our results point towards the opposite, showing that cause and effect may have been reversed. Here, we find that hydrofracture causes rapidly draining lakes to drain before they reach the larger sizes of the non-rapidly draining lakes. In addition, we find no correlation between rapidly draining lake area or volume and local ice thickness (although this correlation does exist for non-rapidly draining lakes), suggesting that rapidly draining lake area and volume do not scale according to ice thickness, but that the incidence of hydrofracture (presumably driven by a different control altogether) limits rapidly draining lake areas and volumes (Sections 3.3 and 4.1). These results agree with the lack of a direct relationship between the lake volume for rapidly draining lakes and the local ice thickness identified in previous work (e.g. Williamson and others, 2017; their fig. 15).

To examine this relationship further, we calculate the 'fracture areas', defined as the individual lake water volume divided by the local ice thickness, following Banwell and others (2013, 2016) and Arnold and others (2014). We find that the fracture areas are higher for non-rapidly draining lakes than rapidly draining lakes: at Paakitsoq, the mean fracture area for rapidly draining lakes is 600 m^2 ($\sigma = 572$ m^2) compared with the mean fracture area for non-rapidly draining lakes of 2002 m^2 ($\sigma = 5084$ m^2); at Store Glacier, the mean fracture area for rapidly draining lakes is 663 m^2 ($\sigma = 594$ m^2) compared with a mean fracture area for non-rapidly draining lakes of 734 m^2 ($\sigma = 919$ m^2). These values show wide scatter across and between the study regions, supporting the idea that including a fracture area within models of the GrIS's surface hydrology is unlikely to be able to reproduce the precise locations and timings of rapid lake drainage, just their broad-scale patterns across the ice sheet (Arnold and others, 2014).

While there is a difference between the rapidly draining and non-rapidly draining lake areas ($p < 0.05$) and volumes ($p = 0.54$) for the reasons explained above, the two lake types are statistically similar for the other hydrological factors (either individually or when combined into PCs). This indicates that the local, hydrological factors of individual lakes are unimportant in hydrofracture initiation. The fact that lake areas are significantly different between the two lake types, but lake volumes and depths are not (with 95% statistical confidence), may be due to the greater uncertainties associated with calculating lake water depth compared with lake area from MODIS imagery, possibly an effect of MODIS's coarse resolution. The FAST algorithm's depth-calculation method tends to report smaller values for the highest water depths compared with those derived from Landsat 8 imagery (Williamson and others, 2017). This might have resulted in the two lake types appearing statistically similar even though they were not. Using a finer-spatial resolution satellite record (such as the Sentinel-2 Multispectral Instrument (MSI), perhaps combined with Landsat 8 images) might overcome this issue, allowing a clearer conclusion to be reached on whether non-rapidly draining lakes, as well as covering

https://doi.org/10.1017/jog.2018.8 Published online by Cambridge University Press

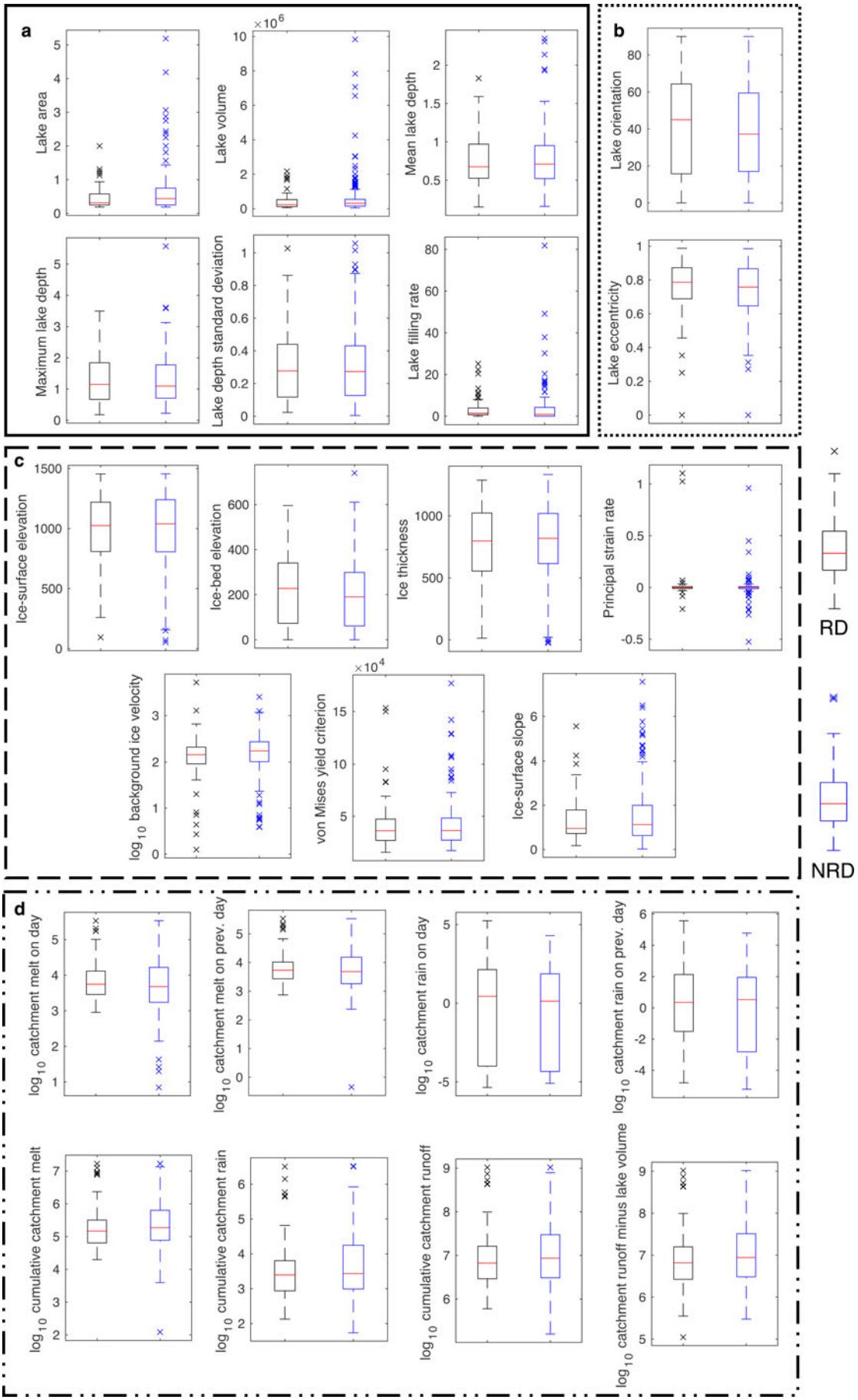

Fig. 4. Boxplots highlighting the similarity of the potential hydrofracture controlling factors for rapidly draining (RD) and non-rapidly draining (NRD) lakes for each factor category (Table 2): (a) hydrological, (b) morphological, (c) glaciological, and (d) SMB. On each boxplot, the red solid line shows the median, the box's upper and lower edges show, respectively, the upper and lower quartiles, the whisker lengths show ± 2.7 σ from the arithmetic mean, and the crosses show values outside of this range. Some data were log-transformed (to the base 10) for presentation purposes only.

https://doi.org/10.1017/jog.2018.8 Published online by Cambridge University Press

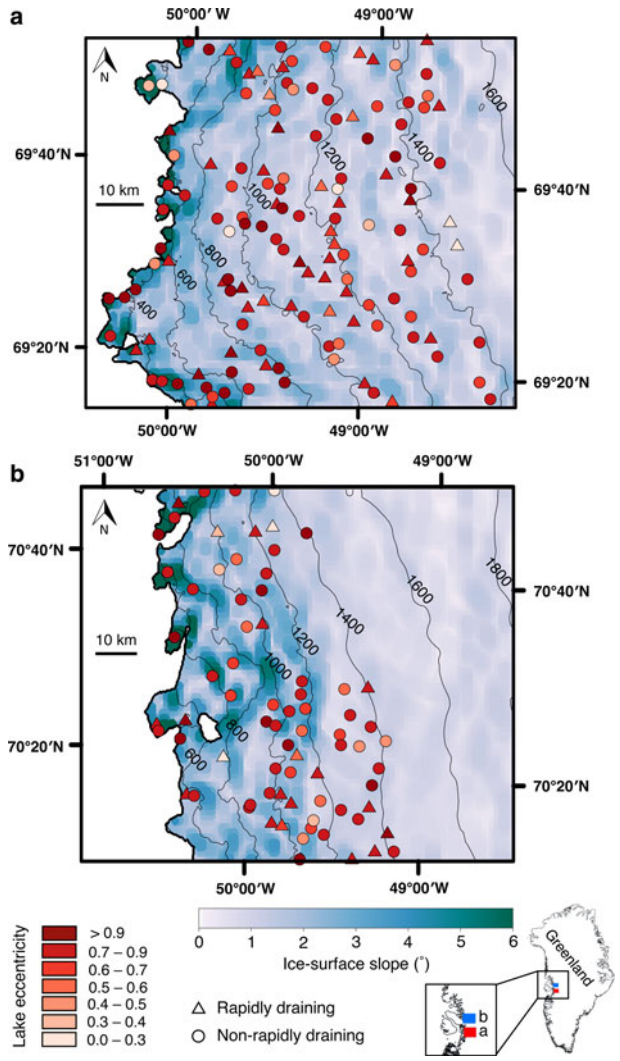

Fig. 5. The locations of rapidly draining (triangles) and non-rapidly draining (circles) lakes within the (a) Paakitsoq and (b) Store Glacier regions of West Greenland (inset) overlying the ice-surface slopes, showing steeper slopes towards the ice margin. Colour coding shows the lake eccentricity on the day of drainage for rapidly draining lakes and on the day when lakes reached their maximum extent for non-rapidly draining lakes. A lake eccentricity value of 0 would indicate a perfect circle and a value of 1 would indicate a line segment. The thick black lines on both panels delineate the GrIS margin from Howat and others (2014). Note the difference in horizontal scale between the two panels.

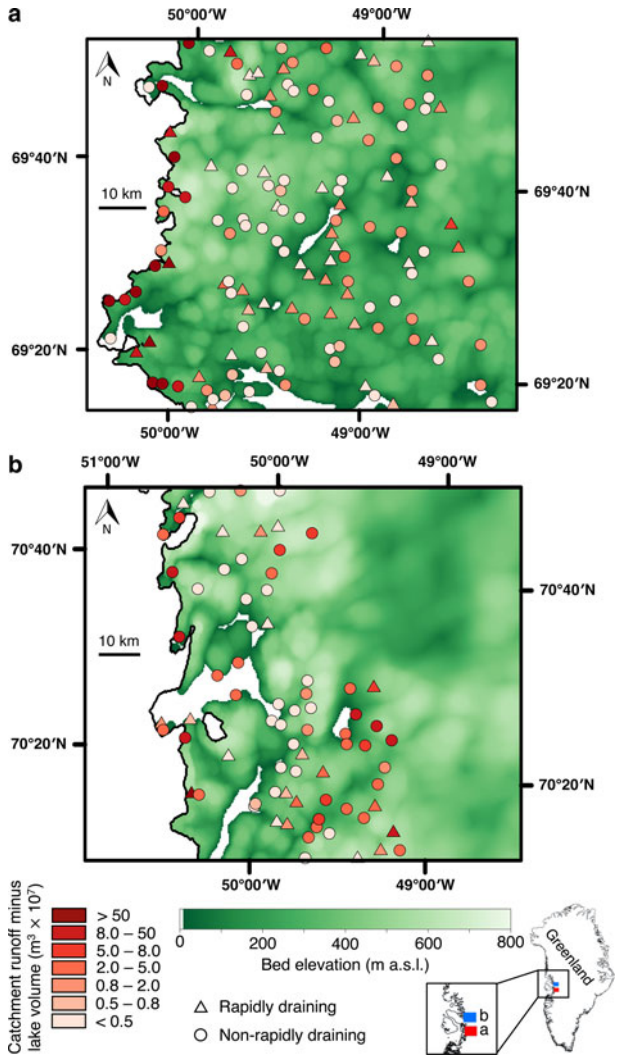

Fig. 6. The locations of rapidly draining (triangles) and non-rapidly draining (circles) lakes within the (a) Paakitsoq and (b) Store Glacier regions of West Greenland (inset) overlying the ice-sheet bed elevation derived from Morlighem and others (2014). Colour coding shows the difference between the cumulative runoff in the catchment, derived from Noël and others (2016), and the lake volume, derived as described in Section 2.1, on the date of drainage for rapidly draining lakes and on the date when lakes reached their maximum extent for non-rapidly draining lakes. The thick black lines on both panels delineate the GrIS margin from Howat and others (2014), and white areas within the ice-sheet area show regions that are at or below mean sea level (i.e. ⩽0 m a.s.l.). Note the difference in horizontal scale between the two panels.

larger areas and containing higher water volumes, also contain deeper water than rapidly draining lakes.

4.2.2. *Morphological factors*

The rapidly draining and non-rapidly draining lakes are similar in terms of their shapes and orientations, showing no link between these properties and the propensity for rapid lake drainage. This indicates that the distribution of the water load on the ice-sheet surface (i.e. whether it is more elongate or circular, and/or whether it is aligned more or less perpendicular or parallel to average ice-flow direction), is unimportant for hydrofracture initiation. This may be because the variation in load distribution is too small relative to the ice thickness to affect the hydrostatic-pressure potential, which possibly explains why we also find no statistically significant difference between the mean filling rates and the likelihood of hydrofracture.

4.2.3. *Glaciological factors*

Our results show that rapidly draining and non-rapidly draining lakes are similar in terms of the glaciological factors investigated. We included the long-term average winter stress field as a potential control on hydrofracture since higher temporal-resolution summer ice-velocity or strain-rate data were not available. While this was useful for defining the long-term average strain regime across each lake basin (which we hypothesised might be a first-order control on hydrofracture), we find no evidence that hydrofracture

https://doi.org/10.1017/jog.2018.8 Published online by Cambridge University Press

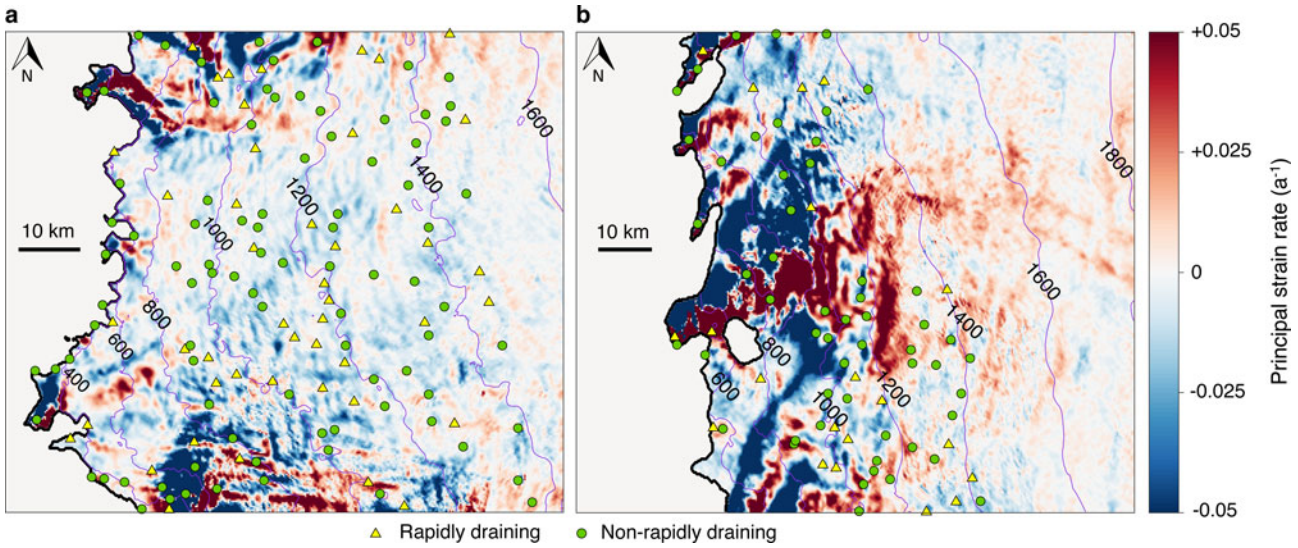

Fig. 7. The variation in the ice-surface principal strain rate across the (a) Paakitsoq and (b) Store Glacier regions, with the locations of rapidly draining (yellow triangles) and non-rapidly draining (green circles) lakes shown. Panels are equivalent to those in Figures 1, 2, 5 and 6. Positive principal strain rates indicate areas undergoing extension and negative ones indicate compression. The thick black lines on both panels delineate the ice-sheet edge and the purple contour lines show ice-surface elevations (m a.s.l.) from Howat and others (2014). The high principal strain rates observed close to the central portion of the ice margin in (b) result from the fast flow rates of the floating tongue of the marine-terminating Store Glacier. Note the difference in horizontal scale between the two panels.

is controlled by the background winter stress or strain field. Existing research has only shown the degree of compression across a lake basin (e.g. Doyle and others, 2013), but has not considered whether the magnitude of the tensor affects the lake's likelihood of drainage, and we did not find support for this idea here. Moreover, we do not see that the background strain or velocity data scales with the rapidly draining lake areas or volumes (Section 3.3), suggesting that a threshold for rapidly draining lake area or volume cannot be linked to the local strain rate or ice velocity. Thus, we have no evidence that including the background stress regime in GrIS surface-hydrology models will improve their ability to predict rapid lake drainage. However, perhaps it is only the deviation from this long-term stress field that is important, resulting, for example, from surface meltwater reaching the bed via a nearby crevasse or moulin, perturbing the horizontal or vertical velocity or stress field beneath a lake basin (Stevens and others, 2015). We attempted to account for this process within our study by including the difference between the cumulative runoff in the lake's catchment and the lake's water volume, but also found negative results (Section 4.2.4).

4.2.4. *SMB factors*

Finally, the two lake types cannot be distinguished statistically on the basis of the SMB factors examined; we find no tendency for rapidly draining lakes to have different meltwater, rain and

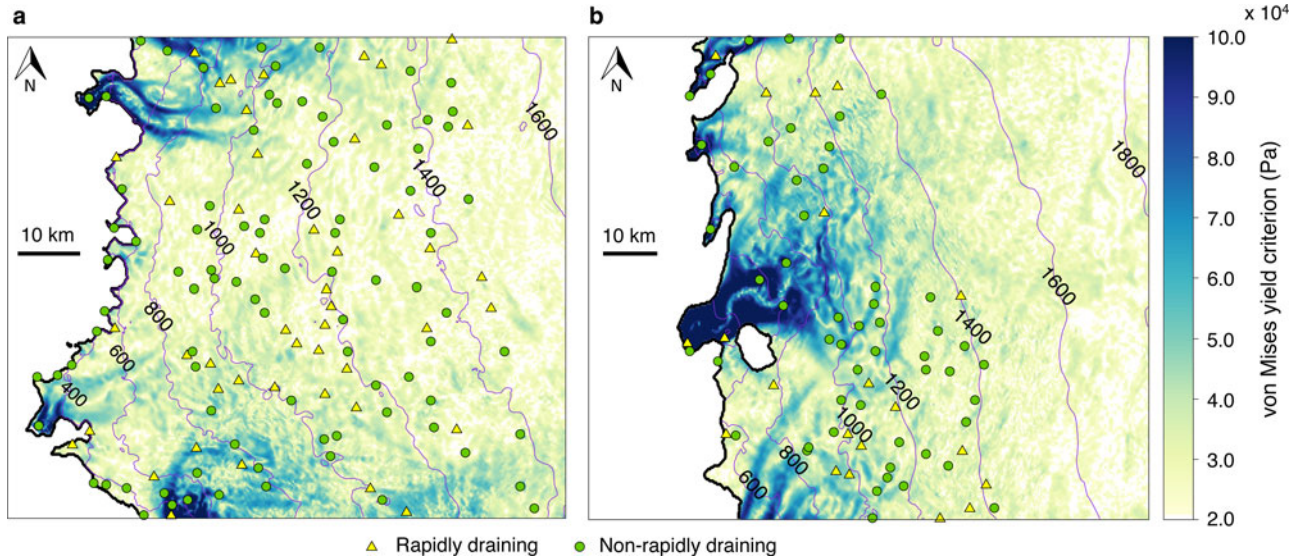

Fig. 8. The variation in the von Mises yield criterion across the (a) Paakitsoq and (b) Store Glacier regions, with the locations of rapidly draining (yellow triangles) and non-rapidly draining (green circles) lakes shown. Panels are equivalent to those in Figures 1, 2, 5 and 6. The thick black lines on both panels delineate the ice-sheet edge and the purple contours show ice-surface elevations (m a.s.l.) from Howat and others (2014). Note the difference in horizontal scale between the two panels.

https://doi.org/10.1017/jog.2018.8 Published online by Cambridge University Press

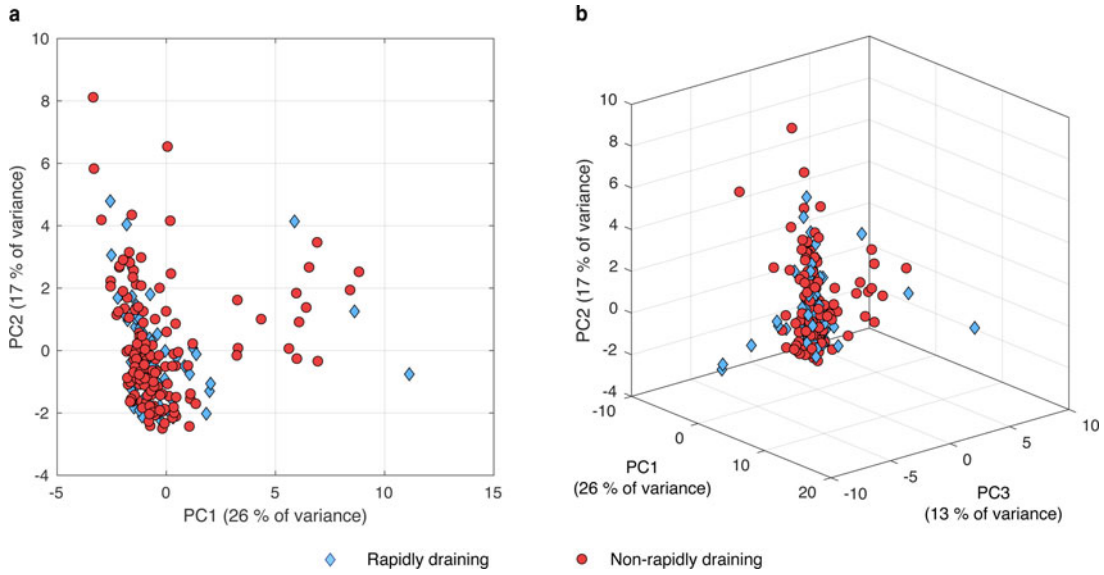

Fig. 9. PC scores for (a) PCs 1 and 2, and (b) PCs 1–3 for rapidly draining (blue diamonds) and non-rapidly draining (red circles) lakes for PCA conducted on all of the potential controlling factors (Table 2) included in the analysis (see Table S2 for eigenvectors). The percentage values labelled on the axes indicate the amount of variance in the data explained by each PC. The tight clustering of the rapidly draining and non-rapidly draining lake PC scores shows the statistical similarity of the potential controlling factors for the two lake types. For individual PCA plots for each category of potential controlling factor (Table 2), see Figures S5–S7.

runoff quantities within their ice-surface catchments. The key rationale for including these factors was because previous work had found that water input to the ice-sheet bed nearby to a lake initiated hydrofracture (Stevens and others, 2015), so we used these SMB data as proxies for this process. Moreover, we specifically attempted to measure the input of water to the bed near to a lake by calculating the total melt in a lake's catchment minus the individual lake volume, but we find no support within our work for the lake-drainage mechanism observed by Stevens and others (2015). However, we did observe a weak positive correlation between the melt, rain and runoff quantities and non-rapidly draining lake area and volume, even though the same correlations did not apply to rapidly draining lakes. This indicates that, for rapidly draining lakes, lake area and volume may not be dependent on these factors, or that they drain before the controls become manifest.

Even though we were unable to corroborate the findings of Stevens and others (2015), that the input of water to the ice-sheet bed close to a lake is a precursor to hydrofracture, for a greater lake sample across the GrIS, this may reflect the coarse resolution of the MODIS imagery (250 m) and the RACMO2.3 grid (1 km) used in this study. The important meltwater-generation and surface-routing processes within lake catchments may operate at too fine a scale to be resolved with these data. Further studies that model or observe surface-meltwater production and its routing at spatial resolutions of metres to tens of metres and combine this information with ice-surface strain rates measured at hourly to daily temporal resolutions would be helpful for examining the influence of water delivery to the ice-sheet bed close to lakes in better detail. This objective could potentially be addressed using either higher-resolution remote-sensing imagery (e.g. WorldView, Sentinel-1 Synthetic Aperture Radar or Sentinel-2 MSI) or more field studies monitoring individual lakes and their catchments, which would generate data at a spatial resolution comparable with that of the size of a fracture formed by rapid lake drainage.

Table 5. Results of unpaired Student's *t*-tests (for each category of controlling factor from Table 2, as well as for all of the 23 potential controlling factors simultaneously, shown within the 'All' category) for the rapidly draining and non-rapidly draining lakes scored for the first three PCs. None of the results are significant at above the 95% confidence interval ($p < 0.05$). See Table S2 for the eigenvectors for the first three PCs

Potential controlling factor category	PC number	*t* value	*p* value
Hydro-morphological	1	−0.388	0.698
	2	−0.220	0.826
	3	−0.068	0.946
Glaciological	1	−1.294	0.197
	2	0.056	0.956
	3	0.945	0.346
SMB	1	−0.935	0.926
	2	0.257	0.798
	3	0.416	0.678
All	1	−1.342	0.181
	2	0.082	0.935
	3	0.638	0.524

4.3. Reasons for this study's negative results and suggestions for future work

Here, we offer three explanations for which our study might not have found causal links between the potential controlling factors and hydrofracture, and suggest how these might be addressed with further research. First, although our EDA included many of the factors that we thought might be important in controlling hydrofracture (with the choice guided by previous research), other potential controls may have been overlooked. It is conceivable, therefore, that there *is* a control on hydrofracture that could be detected using our approach, but that we simply did not identify its potential at the outset. Alternatively, it is possible that a control is

https://doi.org/10.1017/jog.2018.8 Published online by Cambridge University Press

Table 6. Statistically significant correlations identified between non-rapidly draining (NRD) and rapidly draining (RD) lake area or volume (the dependent variables) and the other potential controlling factors (the independent variables). Independent variables are labelled with their category of potentially controlling factor (see Table 2): glaciological (G), morphological (M) and SMB. ρ is the Spearman's rank correlation coefficient, with negative correlations highlighted in italicised font. p is the calculated probability, with all correlations shown significant at above the 95% confidence interval (i.e. $p < 0.05$) and those shown in bold text significant at above the 99% confidence interval (i.e. $p < 0.01$)

Dependent variable	Independent variable	ρ	p
NRD lake area	Ice-bed elevation (G)	*−0.208*	0.012
NRD lake area	Ice thickness (G)	0.185	0.026
NRD lake volume	Ice thickness (G)	0.203	0.015
NRD lake volume	Ice-surface slope (G)	*−0.184*	0.027
NRD lake volume	Lake eccentricity (M)	*−0.176*	0.035
NRD lake area	Cumulative melt within catchment (SMB)	0.216	**0.009**
NRD lake volume	Cumulative melt within catchment (SMB)	0.176	0.035
NRD lake area	Cumulative rain within catchment (SMB)	0.219	**0.008**
NRD lake volume	Cumulative rain within catchment (SMB)	0.198	0.017
NRD lake area	Cumulative runoff within catchment (SMB)	0.262	**0.002**
NRD lake volume	Cumulative runoff within catchment (SMB)	0.219	**0.008**
NRD lake area	Difference between cumulative catchment runoff and lake volume (SMB)	0.167	0.045
RD lake area	Ice-bed elevation (G)	*−0.249*	0.039

important but that it was not in summer 2014 within the study regions; further investigations for other sectors of the GrIS and in additional years would therefore help to validate our negative results. Second, the interplay between some of the controls that we did identify may be too complex to be elicited at the spatial and temporal scales used in this study. Remote sensing and SMB model outputs over finer grids and time steps may overcome this problem, or perhaps the control(s) might only be found from more field-based studies of individual or groups of lakes (Das and others, 2008; Doyle and others, 2013; Tedesco and others, 2013; Stevens and others, 2015). With continuing improvements to the availability and resolution of remotely sensed data (such as ice-bed topography (e.g. Morlighem and others, 2017) or ice-velocity data), future studies that use a similar EDA approach to this one alongside these new datasets might be better able to reveal the control(s) on hydrofracture. Third, there may be a strong stochastic element to rapid lake drainage, which would explain the statistical similarity between the lake types observed in this study and which may help to explain why some lakes change their mode of drainage interannually (Selmes and others, 2013; Fitzpatrick and others, 2014). For example, hydrofracture might only be possible if pre-existing weaknesses exist in the ice beneath a lake basin, which can then be exploited by a load on the ice surface (Catania and others, 2008). This would consequently make rapid lake drainage appear random. Without being able to include these very site-specific processes and ice-sheet features, which relate to the complex strain history up-glacier of a lake, it may be difficult to predict rapid lake drainage with confidence. A more detailed examination of such features as well as the strain history up-glacier of a lake would therefore be helpful.

5. CONCLUSIONS

Previous studies have suggested that rapid lake drainage is a key contributor to the GrIS's negative mass balance and may become more widespread in the future as lakes continue to advance inland. Despite this, the precise controls on rapid lake drainage remain uncertain, having not been examined comprehensively within existing research. Our aim here was therefore to address this shortfall by conducting a comprehensive, statistically robust EDA of various potential controls on hydrofracture for a large sample of rapidly draining and non-rapidly draining lakes in West Greenland.

Our results, however, did not indicate any clear links between the incidence of hydrofracture and the potential controlling factors examined for the two study regions in summer 2014. This means that we cannot recommend an empirically supported alternative to the fracture area threshold parameter in use within current surface-hydrology models of the GrIS (Banwell and others, 2013, 2016; Arnold and others, 2014; Clason and others, 2015; Koziol and others, 2017), but nor can we provide evidence to support the use of a fracture area threshold parameter in future surface-hydrology models if the aim is to predict the precise magnitude and timing of individual rapid lake-drainage events. Here, we showed that rapid lake drainage controls lake size, and not the reverse, directly contradicting the use of a fracture area threshold in such models. Using a deterministic basis to predict precisely when and where rapid lake drainage will occur therefore remains the weakest component of GrIS hydrology models, despite recent work showing the importance of the lake-drainage process for the evolution of subglacial drainage (Banwell and others, 2016). Future work could focus on incorporating some of the potential controls identified here into supraglacial-hydrology models of the GrIS, and testing their ability to reproduce empirical observations with these controls included. These improvements to surface-hydrology models are necessary to provide more realistic inputs to SMB models (requiring knowledge of lake locations and their duration on the GrIS surface to determine the amount of enhanced surface ablation), and to coupled subglacial hydrology-ice flow models (requiring knowledge of the timing and magnitude of meltwater deliveries to the ice-sheet bed to determine ice-dynamic impacts). Therefore, if better knowledge were gained of the controls on the hydrofracture process, these deterministic models could be confidently forced with future climate projections; this would generate robust patterns of rapid lake drainage across the GrIS, ultimately helping to improve forecasts of water

https://doi.org/10.1017/jog.2018.8 Published online by Cambridge University Press

runoff, dynamic ice discharge and thus sea-level rise from the GrIS over the coming century.

AUTHOR CONTRIBUTIONS

All authors conceived the study. AGW designed the methodological approach, processed the data and undertook the analysis under supervision from the other authors. All authors were involved in interpreting the results. AGW wrote the manuscript, with all authors commenting on and editing it. AGW, with input from ICW, revised the manuscript following reviewer and editorial comments.

SUPPLEMENTARY MATERIAL

The supplementary material for this article can be found at https://doi.org/10.1017/jog.2018.8

ACKNOWLEDGEMENTS

AGW was funded by a UK Natural Environment Research Council PhD studentship (NE/L002507/1) awarded through the Cambridge Earth System Science Doctoral Training Partnership. AFB was funded by a Leverhulme/Newton Trust Early Career Fellowship (ECF-2014-412). We thank Brice Noël for providing the RACMO2.3 data, and Conrad Koziol for providing the original MATLAB function to calculate the von Mises yield criterion from the ice-velocity data. We are grateful to Nick Selmes for discussions during the conception of the study, and to Jerome Neufeld and Stephen Kissler for their early advice regarding the appropriate statistical techniques for the research. Finally, we thank Ted Scambos (the Scientific Editor) and one anonymous reviewer for their comments that improved the manuscript.

REFERENCES

Alley RB, Dupont TK, Parizek BR and Anandakrishnan S (2005) Access of surface meltwater to beds of sub-freezing glaciers: preliminary insights. *Ann. Glaciol.*, **40**, 8–14 (https://doi.org/10.3189/172756405781813483)

Andrews LC and 7 others (2014) Direct observations of evolving subglacial drainage beneath the Greenland ice sheet. *Nature*, **514**(7520), 80–83 (https://doi.org/10.1038/nature13796)

Arnold NS, Banwell AF and Willis IC (2014) High-resolution modelling of the seasonal evolution of surface water storage on the Greenland ice sheet. *Cryosphere*, **8**(4), 1149–1160 (https://doi.org/10.5194/tc-8-1149-2014)

Banwell AF, Arnold NS, Willis IC, Tedesco M and Ahlstrøm AP (2012) Modeling supraglacial water routing and lake filling on the Greenland ice sheet. *J. Geophys. Res.: Earth Surf.*, **117**, F04012 (https://doi.org/10.1029/2012JF002393)

Banwell AF, Willis IC and Arnold NS (2013) Modeling subglacial water routing at Paakitsoq, W Greenland. *J. Geophys. Res.: Earth Surf.*, **118**(3), 1282–1295 (https://doi.org/10.1002/jgrf.20093)

Banwell AF and 5 others (2014) Supraglacial lakes on the Larsen B ice shelf, Antarctica, and at Paakitsoq, west Greenland: a comparative study. *Ann. Glaciol.*, **55**(66), 1–8 (https://doi.org/10.3189/2014AoG66A049)

Banwell A, Hewitt I, Willis I and Arnold N (2016) Moulin density controls drainage development beneath the Greenland ice sheet. *J. Geophys. Res.: Earth Surf.*, **121**(12), 2248–2269 (https://doi.org/10.1002/2015jf003801)

Bartholomew I and 5 others (2010) Seasonal evolution of subglacial drainage and acceleration in a Greenland outlet glacier. *Nat. Geosci.*, **3**(6), 408–411 (https://doi.org/10.1038/ngeo863)

Bartholomew ID and 6 others (2011a) Seasonal variations in Greenland ice sheet motion: inland extent and behaviour at higher elevations. *Earth Planet. Sci. Lett.*, **307**(3), 271–278 (https://doi.org/10.1016/j.epsl.2011.04.014)

Bartholomew I and 6 others (2011b) Supraglacial forcing of subglacial drainage in the ablation zone of the Greenland ice sheet. *Geophys. Res. Lett.*, **38**, L08502 (https://doi.org/10.1029/2011GL047063)

Bartholomew I and 5 others (2012) Short-term variability in Greenland ice sheet motion forced by time-varying meltwater drainage: implications for the relationship between subglacial drainage system behavior and ice velocity. *J. Geophys. Res.: Earth Surf.*, **117**, F03002 (https://doi.org/10.1029/2011jf002220)

Boon S and Sharp M (2003) The role of hydrologically-driven ice fracture in drainage system evolution on an Arctic glacier. *Geophys. Res. Lett.*, **30**, L018034 (https://doi.org/10.1029/2003GL018034)

Bougamont M and 5 others (2014) Sensitive response of the Greenland ice sheet to surface melt drainage over a soft bed. *Nat. Comm.*, **5**(5052) (https://doi.org/10.1038/ncomms6052)

Box JE and Ski K (2007) Remote sounding of Greenland supraglacial melt lakes: implications for subglacial hydraulics. *J. Glaciol.*, **53**(181), 257–265 (https://doi.org/10.3189/172756507782202883)

Catania GA, Neumann TA and Price SF (2008) Characterizing englacial drainage in the ablation zone of the Greenland ice sheet. *J. Glaciol.*, **54**(187), 567–578 (https://doi.org/10.3189/002214308786570854)

Chandler DM and 11 others (2013) Evolution of the subglacial drainage system beneath the Greenland ice sheet revealed by tracers. *Nat. Geosci.*, **6**(3), 195–198 (https://doi.org/10.1038/ngeo1737)

Chen C, Howat IM and de la Peña S (2017) Formation and development of supraglacial lakes in the percolation zone of the Greenland ice sheet. *J. Glaciol.*, **63**, 847–853 (https://doi.org/10.1017/jog.2017.50)

Chu VW (2014) Greenland ice sheet hydrology: a review. *Prog. in Phys. Geogr.*, **38**(1), 19–54 (https://doi.org/10.1177/0309133313507075)

Clason C, Mair DW, Burgess DO and Nienow PW (2012) Modelling the delivery of supraglacial meltwater to the ice/bed interface: application to southwest Devon ice cap, Nunavut, Canada. *J. Glaciol.*, **58**(208), 361–374 (https://doi.org/10.3189/2012JoG11J129)

Clason CC and 6 others (2015) Modelling the transfer of supraglacial meltwater to the bed of leverett glacier, southwest Greenland. *Cryosphere*, **9**, 123–138 (https://doi.org/10.5194/tc-9-123-2015)

Colgan W and 7 others (2011a) The annual glaciohydrology cycle in the ablation zone of the Greenland ice sheet: part 1. Hydrology model. *J. Glaciol.*, **57**(204), 697–709 (https://doi.org/10.3189/002214311797409668)

Colgan W and 7 others (2011b) An increase in crevasse extent, west Greenland: hydrologic implications. *Geophys. Res. Lett.*, **38**, L18503 (https://doi.org/10.1029/2011GL048491)

Cooley SW and Christoffersen P (2017) Observation bias correction reveals more rapidly draining lakes on the Greenland ice sheet. *J. Geophys. Res.: Earth Surf.*, **122**, 1867–1881 (https://doi.org/10.1002/2017JF004255)

Cowton T and 7 others (2013) Evolution of drainage system morphology at a land-terminating Greenlandic outlet glacier. *J. Geophys. Res.: Earth Surf.*, **118**(1), 29–41 (https://doi.org/10.1029/2012jf002540)

Das SB and 6 others (2008) Fracture propagation to the base of the Greenland ice sheet during supraglacial lake drainage. *Science*, **320**(5877), 778–781 (https://doi.org/10.1126/science.1153360)

Dow CF, Kulessa B, Rutt IC, Doyle SH and Hubbard A (2014) Upper bounds on subglacial channel development for interior regions of the Greenland ice sheet. *J. Glaciol.*, **60**(224), 1044–1052 (https://doi.org/10.3189/2014JoG14J093)

Doyle SH and 9 others (2013) Ice tectonic deformation during the rapid in situ drainage of a supraglacial lake on the Greenland ice sheet. *Cryosphere*, **7**(1), 129–140 (https://doi.org/10.5194/tc-7-129-2013)

Doyle SH and 6 others (2014) Persistent flow acceleration within the interior of the Greenland ice sheet. *Geophys. Res. Lett.*, **41**, 899–905 (https://doi.org/10.1002/2013GL058933)
Everett A and 10 others (2016) Annual down-glacier drainage of lakes and water-filled crevasses at Helheim glacier, southeast Greenland. *J. Geophys. Res.: Earth Surf.*, **121**(10), 1819–1833 (https://doi.org/10.1002/2016JF003831)
Fahnestock M and 5 others (2016) Rapid large-area mapping of ice flow using Landsat 8. *Remote Sens. Environ.*, **185**, 84–94 (https://doi.org/10.1016/j.rse.2015.11.023)
Fitzpatrick AAW and 8 others (2013) Ice flow dynamics and surface meltwater flux at a land-terminating sector of the Greenland ice sheet. *J. Glaciol.*, **59**(216), 687–696 (https://doi.org/10.3189/2013JoG12J143)
Fitzpatrick AAW and 9 others (2014) A decade (2002–2012) of supraglacial lake volume estimates across Russell glacier, west Greenland. *Cryosphere*, **8**(1), 107–121 (https://doi.org/10.5194/tc-8-107-2014)
Gledhill LA and Williamson AG (2018) Inland advance of supraglacial lakes in north-west Greenland under recent climatic warming. *Ann. Glaciol.* (https://doi.org/10.1017/aog.2017.31)
Greenwood SL, Clason CC, Helanow C and Margold M (2016) Theoretical, contemporary observational and palaeo-perspectives on ice sheet hydrology: processes and products. *Earth Sci. Rev.*, **155**, 1–27 (https://doi.org/10.1016/j.earscirev.2016.01.010)
Hoffman MJ, Catania GA, Neumann TA, Andrews LC and Rumrill JA (2011) Links between acceleration, melting, and supraglacial lake drainage of the western Greenland ice sheet. *J. Geophys. Res.: Earth Surf.*, **116**(F4) (https://doi.org/10.1029/2010JF001934)
Howat IM, de la Peña S, van Angelen JH, Lenaerts TM and van den Broeke MR (2013) Brief communication: "expansion of meltwater lakes on the Greenland ice sheet". *Cryosphere*, **7**(1), 201–204 (https://doi.org/10.5194/tc-7-201-2013)
Howat IM, Negrete A and Smith BE (2014) The Greenland Ice Mapping Project (GIMP) land classification and surface elevation data sets. *Cryosphere*, **8**(4), 1509–1518 (https://doi.org/10.5194/tc-8-1509-2014)
Irvine-Fynn TDL, Hodson AJ, Moorman BJ, Vatne G and Hubbard AL (2011) Polythermal glacier hydrology: a review. *Rev. Geophys.*, **49**, 1–37 (https://doi.org/10.1029/2010RG000350)
Johansson AM, Jansson P and Brown IA (2013) Spatial and temporal variations in lakes on the Greenland ice sheet. *J. Hydrol.*, **476**, 314–320 (https://doi.org/10.1016/j.jhydrol.2012.10.045)
Jolliffe IT (2002) *Principal component analysis*. Springer, New York
Joughin I and 5 others (2008) Seasonal speedup along the western flank of the Greenland ice sheet. *Science*, **320**(5877), 781–783 (https://doi.org/10.1126/science.1153288)
Joughin I, Smith BE, Howat IM, Scambos T and Moon T (2010) Greenland flow variability from ice-sheet-wide velocity mapping. *J. Glaciol.*, **56**(197), 415–430 (https://doi.org/10.3189/002214310792447734)
Joughin I and 9 others (2013) Influence of ice-sheet geometry and supraglacial lakes on seasonal ice-flow variability. *Cryosphere*, **7** 1185–1192 (https://doi.org/10.5194/tc-7-1185-2013)
Joughin I, Smith BE, Howat IM, Moon T and Scambos T (2016) A SAR record of early 21st century change in Greenland. *J. Glaciol.*, **62**(231), 62–71 (https://doi.org/10.1017/jog.2016.10)
Koziol C, Arnold N, Pope A and Colgan W (2017) Quantifying supraglacial meltwater pathways in the Paakitsoq region, west Greenland. *J. Glaciol.*, **63**(239), 464–476 (https://doi.org/10.1017/jog.2017.5)
Krawczynski MJ, Behn MD, Das SB and Joughin I (2009) Constraints on the lake volume required for hydro-fracture through ice sheets. *Geophys. Res. Lett.*, **36**(10) (https://doi.org/10.1029/2008GL036765)
Kulessa B and 10 others (2017) Seismic evidence for complex sedimentary control of Greenland ice sheet flow. *Sci. Adv.*, **3**, 1–8 (https://doi.org/10.1126/sciadv.1603071)
Lampkin DJ and VanderBerg J (2011) A preliminary investigation of the influence of basal and surface topography on supraglacial lake distribution near Jakobshavn Isbrae, western Greenland. *Hydrol. Process.*, **25**, 3347–3355 (https://doi.org/10.1002/hyp.8170)
Leeson AA and 7 others (2013) A comparison of supraglacial lake observations derived from MODIS imagery at the western margin of the Greenland ice sheet. *J. Glaciol.*, **59**(218), 1179–1188 (https://doi.org/10.3189/2013JoG13J064)
Leeson AA and 6 others (2015) Supraglacial lakes on the Greenland ice sheet advance inland under warming climate. *Nat. Clim. Change*, **5**(1), 51–55 (https://doi.org/10.1038/nclimate2463)
Liang Y and 7 others (2012) A decadal investigation of supraglacial lakes in west Greenland using a fully automatic detection and tracking algorithm. *Remote Sens. Environ.*, **123**, 127–138 (https://doi.org/10.1016/j.rse.2012.03.020)
Lüthje M, Pedersen LT, Reeh N and Greuell W (2006) Modelling the evolution of supraglacial lakes on the West Greenland ice-sheet margin. *J. Glaciol.*, **52**(179), 608–618 (https://doi.org/10.3189/172756506781828386)
Lüthi MP and 7 others (2015) Heat sources within the Greenland ice sheet: dissipation, temperature, paleo-firn and cryo-hydrologic warming. *Cryosphere*, **9**, 245–253 (https://doi.org/10.5194/tc-9-245-2015)
Mayaud JR, Banwell AF, Arnold NS and Willis IC (2014) Modeling the response of subglacial drainage at Paakitsoq, west Greenland, to 21st century climate change. *J. Geophys. Res.: Earth Surf.*, **119**, 2619–2634 (https://doi.org/10.1002/2014JF003271)
Meierbachtol T, Harper J and Humphrey N (2013) Basal drainage system response to increasing surface melt on the Greenland ice sheet. *Science*, **341**(6147), 777–779 (https://doi.org/10.1126/science.1235905)
Miles KE, Willis IC, Benedek CL, Williamson AG and Tedesco M (2017) Toward monitoring surface and subsurface lakes on the Greenland ice sheet using Sentinel-1 SAR and Landsat-8 OLI imagery. *Front. Earth Sci.*, **5**(58), 1–17 (https://doi.org/10.3389/feart.2017.00058)
Morlighem M, Rignot E, Mouginot J, Seroussi H and Larour E (2014) Deeply incised submarine glacial valleys beneath the Greenland ice sheet. *Nat. Geosci.*, **7**, 418–422 (https://doi.org/10.1038/ngeo2167)
Morlighem M and 31 others (2017) Bedmachine v3: complete bed topography and ocean bathymetry mapping of Greenland from multibeam echo sounding combined with mass conservation. *Geophys. Res. Lett.*, **44**(21), 11,051–11,061 (https://doi.org/10.1002/2017GL074954)
Morriss BF and 7 others (2013) A ten-year record of supraglacial lake evolution and rapid drainage in west Greenland using an automated processing algorithm for multispectral imagery. *Cryosphere*, **7**(6), 1869–1877 (https://doi.org/10.5194/tc-7-1869-2013)
Nienow PW, Sole AJ, Slater DA and Cowton TR (2017) Recent advances in our understanding of the role of meltwater in the Greenland ice sheet system. *Curr. Clim. Change Rep.*, **3** (https://doi.org/10.1007/s40641-017-0083-9)
Noël B and 6 others (2016) A daily, 1-km resolution data set of downscaled Greenland ice sheet mass balance (1958–2015). *Cryosphere*, **10**, 2361–2377 (https://doi.org/10.5194/tc-10-2361-2016)
Palmer S, Shepherd A, Nienow P and Joughin I (2011) Seasonal speedup of the Greenland ice sheet linked to routing of surface water. *Earth Planet. Sci. Lett.*, **302**, 423–428 (https://doi.org/10.1016/j.epsl.2010.12.037)
Phillips T, Rajaram H and Steffen K (2010) Cryo-hydrologic warming: a potential mechanism for rapid thermal response of ice sheets. *Geophys. Res. Lett.*, **37**(20) (https://doi.org/10.1029/2010GL044397)
Phillips T, Rajaram H, Colgan W, Steffen K and Abdalati W (2013) Evaluation of cryo-hydrologic warming as an explanation for increased ice velocities in the wet snow zone, Sermeq Avannarleq, west Greenland. *J. Geophys. Res.: Earth Surf.*, **118**(3), 1241–1256 (https://doi.org/10.1002/jgrf.20079)
Poinar K and 5 others (2015) Limits to future expansion of surface-melt-enhanced ice flow into the interior of western Greenland.

Geophys. Res. Lett., **42**(6), 1800–1807 (https://doi.org/10.1002/2015GL063192)
Poinar K, Joughin I, Lenaerts JTM and van den Broeke MR (2017) Englacial latent-heat transfer has limited influence on seaward ice flux in western Greenland. *J. Glaciol.*, **63**(237), 1–16 (https://doi.org/10.1017/jog.2016.103)
Pope A and Rees WG (2014a) Impact of spatial, spectral, and radiometric properties of multispectral imagers on glacier surface classification. *Remote Sens. Environ.*, **141**, 1–13 (https://doi.org/10.1016/j.rse.2013.08.028)
Pope A and Rees G (2014b) Using *in situ* spectra to explore Landsat classification of glacier surfaces. *Int. J. Appl. Earth Obs. Geoinf.*, **27**, 42–52 (https://doi.org/10.1016/j.jag.2013.08.007)
Pope A and 6 others (2016) Estimating supraglacial lake depth in west Greenland using Landsat 8 and comparison with other multispectral sensors. *Cryosphere*, **10**, 15–27 (https://doi.org/10.5194/tc-10-15-2016)
Ringnér M (2008) What is principal component analysis? *Nat. Biotechnol.*, **26**(3), 303–304 (https://doi.org/10.1038/nbt0308-303)
Schoof C (2010) Ice-sheet acceleration driven by melt supply variability. *Nature*, **468**(7325), 803–806 (https://doi.org/10.1038/nature09618)
Selmes N, Murray T and James TD (2011) Fast draining lakes on the Greenland ice sheet. *Geophys. Res. Lett.*, **38**, L15501 (https://doi.org/10.1029/2011GL047872)
Selmes N, Murray T and James TD (2013) Characterizing supraglacial lake drainage and freezing on the Greenland ice sheet. *Cryos. Discuss.*, **7**(1), 475–505 (https://doi.org/10.5194/tcd-7-475-2013)
Sergienko OV (2013) Glaciological twins: basally controlled subglacial and supraglacial lakes. *J. Glaciol.*, **59**(213), 3–8 (https://doi.org/10.3189/2013JoG12J040)
Shepherd A and 5 others (2009) Greenland ice sheet motion coupled with daily melting in late summer. *Geophys. Res. Lett.*, **36**, L01501 (https://doi.org/10.1029/2008GL035758)
Sneed WA and Hamilton GS (2007) Evolution of melt pond volume on the surface of the Greenland ice sheet. *Geophys. Res. Lett.*, **34**, L03501 (https://doi.org/10.1029/2006GL028697)
Sole A and 6 others (2013) Winter motion mediates dynamic response of the Greenland ice sheet to warmer summers. *Geophys. Res. Lett.*, **40**(15), 3940–3944 (https://doi.org/10.1002/grl.50764)
Stevens LA and 7 others (2015) Greenland supraglacial lake drainages triggered by hydrologically induced basal slip. *Nature*, **522**(7554), 73–76 (https://doi.org/10.1038/nature14608)
Sundal AV and 5 others (2009) Evolution of supra-glacial lakes across the Greenland ice sheet. *Remote Sens. Environ.*, **113**(10), 2164–2171 (https://doi.org/10.1016/j.rse.2009.05.018)
Sundal AV and 5 others (2011) Melt-induced speed-up of Greenland ice sheet offset by efficient subglacial drainage. *Nature*, **469**(7331), 521–524 (https://doi.org/10.1038/nature09740)
Tedesco M and Steiner S (2011) In-situ multispectral and bathymetric measurements over a supraglacial lake in western Greenland using a remotely controlled watercraft. *Cryosphere*, **5**, 445–452 (https://doi.org/10.5194/tc-5-445-2011)
Tedesco M and 7 others (2012) Measurement and modeling of ablation of the bottom of supraglacial lakes in western Greenland. *Geophys. Res. Lett.*, **39**(2), L02052 (https://doi.org/10.1029/2011GL049882)
Tedesco M and 5 others (2013) Ice dynamic response to two modes of surface lake drainage on the Greenland ice sheet. *Environ. Res. Lett.*, **8**(3), 034007 (https://doi.org/10.1088/1748-9326/8/3/034007)
Tedstone AJ, Nienow PW, Gourmelen N and Sole AJ (2014) Greenland ice sheet annual motion insensitive to spatial variations in subglacial hydraulic structure. *Geophys. Res. Lett.*, **41**, 8910–8917 (https://doi.org/10.1002/2014GL062386)
Tedstone AJ and 5 others (2015) Decadal slowdown of a land-terminating sector of the Greenland ice sheet despite warming. *Nature*, **526**(7575), 692–695 (https://doi.org/10.1038/nature15722)
Tsai VC and Rice JR (2010) A model for turbulent hydraulic fracture and application to crack propagation at glacier beds. *J. Geophys. Res.: Earth Surf.*, **115**, F03007 (https://doi.org/10.1029/2009jf001474)
Tukey JW (1977) *Exploratory data analysis*. Addison-Wesley, Reading, MA.
van de Wal RSW and 6 others (2008) Large and rapid melt-induced velocity changes in the ablation zone of the Greenland ice sheet. *Science*, **321**(5885), 111–113 (https://doi.org/10.1126/science.1158540)
van den Broeke MR, Enderlin EM, Howat IM and Noël BP (2016) On the recent contribution of the Greenland ice sheet to sea level change. *Cryosphere*, **10**(5), 1933–1946 (https://doi.org/10.5194/tc-10-1933-2016)
van der Veen CJ (2007) Fracture propagation as means of rapidly transferring surface meltwater to the base of glaciers. *Geophys. Res. Lett.*, **34**(1), L01501 (https://doi.org/10.1029/2006GL028385)
Vaughan D (1993) Relating the occurrence of crevasses to surface strain rates. *J. Glaciol.*, **39**(132), 255–266 (https://doi.org/10.1017/S0022143000015926)
Williamson AG, Arnold NS, Banwell AF and Willis IC (2017) A Fully Automated Supraglacial lake area and volume Tracking ("FAST") algorithm: development and application using MODIS imagery of west Greenland. *Remote Sens. Environ.*, **196**, 113–133 (https://doi.org/10.1016/j.rse.2017.04.032)
Zwally HJ and 5 others (2002) Surface melt-induced acceleration of Greenland ice-sheet flow. *Science*, **297**(5579), 218–222 (https://doi.org/10.1126/science.1072708)

MS received 1 September 2017 and accepted in revised form 16 January 2018; first published online 4 March 2018